Title

Platelets Contain Tissue Factor Pathway Inhibitor-2 Derived from Megakaryocytes and Inhibits Fibrinolysis*

Journal

Journal of Biological Chemistry, 289(45)

ISSN

0021-9258

Authors

Vadivel, Kanagasabai
Ponnuraj, Sathya-Moorthy
Kumar, Yogesh
et al.

Publication Date

2014-11-01

DOI

10.1074/jbc.m114.569665

Peer reviewed

THE JOURNAL OF BIOLOGICAL CHEMISTRY VOL. 289, NO. 45, pp. 31647–31661, November 7, 2014

Platelets Contain Tissue Factor Pathway Inhibitor-2 Derived from Megakaryocytes and Inhibits Fibrinolysis*

Received for publication, April 27, 2014, and in revised form, September 9, 2014 Published, JBC Papers in Press, September 28, 2014, DOI 10.1074/jbc.M114.569665

Kanagasabai Vadivel[‡1], Sathya-Moorthy Ponnuraj[‡1], Yogesh Kumar[‡1], Anne K. Zaiss[§1,2], Matthew W. Bunce[¶], Rodney M. Camire[¶], Ling Wu[‡], Denis Evseenko[‡], Harvey R. Herschman[§‖], Madhu S. Bajaj[**], and S. Paul Bajaj[‡‖3]

From the [‡]UCLA/Orthopaedic Hospital Department of Orthopaedic Surgery, the [§]Department of Molecular and Medical Pharmacology, the [**]Department of Medicine, Division of Pulmonology and Critical Care, and the [‖]Molecular Biology Institute, UCLA, Los Angeles, California 90095 and the [¶]Department of Pediatrics, Division of Hematology, Children's Hospital of Philadelphia, University of Pennsylvania, Philadelphia, Pennsylvania 19104

Background: TFPI-2 inhibits plasma kallikrein, FXIa, and plasmin, but its concentration in normal plasma is insufficient to inhibit clotting or fibrinolysis.
Results: Platelets contain TFPI-2 derived from megakaryocytes and binds to platelet FV/Va and circulating FV in late pregnancy when plasma TFPI-2 is ~7 nM.
Conclusion: Platelet-derived TFPI-2 regulates intrinsic coagulation and tPA-induced fibrinolysis.
Significance: Platelet-derived TFPI-2 promotes clot stabilization while attenuating intrinsic clotting.

Tissue factor pathway inhibitor-2 (TFPI-2) is a homologue of TFPI-1 and contains three Kunitz-type domains and a basic C terminus region. The N-terminal domain of TFPI-2 is the only inhibitory domain, and it inhibits plasma kallikrein, factor XIa, and plasmin. However, plasma TFPI-2 levels are negligible (≤20 pM) in the context of influencing clotting or fibrinolysis. Here, we report that platelets contain significant amounts of TFPI-2 derived from megakaryocytes. We employed RT-PCR, Western blotting, immunohistochemistry, and confocal microscopy to determine that platelets, MEG-01 megakaryoblastic cells, and bone marrow megakaryocytes contain TFPI-2. ELISA data reveal that TFPI-2 binds factor V (FV) and partially B-domain-deleted FV (FV-1033) with K_d ~9 nM and binds FVa with K_d ~100 nM. Steady state analysis of surface plasmon resonance data reveal that TFPI-2 and TFPI-1 bind FV-1033 with K_d ~36–48 nM and bind FVa with K_d ~252–456 nM. Further, TFPI-1 (but not TFPI-1_{161}) competes with TFPI-2 in binding to FV. These data indicate that the C-terminal basic region of TFPI-2 is similar to that of TFPI-1 and plays a role in binding to the FV B-domain acidic region. Using pull-down assays and Western blots, we show that TFPI-2 is associated with platelet FV/FVa. TFPI-2 (~7 nM) in plasma of women at the onset of labor is also, in part, associated with FV. Importantly, TFPI-2 in platelets and in plasma of pregnant women inhibits FXIa and tissue-type plasminogen activator-induced clot fibrinolysis. In conclusion, TFPI-2 in platelets from normal or pregnant subjects and in plasma from pregnant women binds FV/Va and regulates intrinsic coagulation and fibrinolysis.

Two members of the Kunitz family of inhibitors that are involved in coagulation and fibrinolysis are tissue factor pathway inhibitor type 1 (TFPI-1)[4] and its homologue, TFPI-2 (1, 2). TFPI-2, also known as placental protein 5 (3) or matrix serine protease inhibitor (4), features a domain organization similar to that of TFPI-1 and contains three Kunitz-type domains in tandem with a short N terminus and a very basic C-terminal region. With respect to the vascular system, TFPI-2 inhibition of plasma kallikrein (pKLK), factor XIa (FXIa), and plasmin are of primary importance (5–9). Notably, TFPI-2 inhibits FVIIa/tissue factor (TF) very poorly, with K_i ~1 μM (5, 10, 11), and has very little inhibitory activity toward tissue-type plasminogen activator (tPA), urokinase-type plasminogen activator (uPA), activated protein C, tissue kallikreins, leukocyte elastase, and thrombin (5, 11, 12). The inhibitory activity of TFPI-2 resides in its N-terminal Kunitz domain 1 (KD1-WT); the other two domains have no inhibitory activity. In contrast, TFPI-1 inhibits FXa via its second domain and FVIIa/TF via its first domain with K_i values in the subnanomolar range; the third domain of TFPI-1 has no known inhibitory activity (1, 13). Thus, TFPI-2 essentially inhibits intrinsic clotting (pKLK and FXIa) as well as plasmin, whereas TFPI-1 inhibits extrinsic clotting (FVIIa/TF and FXa).

The plasminogen-plasmin system is involved in many biological processes, including fibrinolysis and degradation of the extracellular matrix (ECM) (14, 15). The ECM degradation is partly attributable to uPA (complex with uPA receptor)-mediated activation of plasminogen bound to its cell surface recep-

* This work was supported, in whole or in part, by National Institutes of Health, NHLBI, Grants RO1HL88010 (to R. M. C.), R21HL89661 (to M. S. B.), and R01HL36365 (to S. P. B.). This work was also supported by Department of Defense Grant OR12016 (to D. E.).
[1] These authors contributed equally to this work.
[2] Recipient of an American Society of Hematology Scholar Award.
[3] To whom correspondence may be addressed: Dept. of Orthopaedic Surgery, David Geffen School of Medicine, University of California, Los Angeles, CA 90095. Tel.: 310-825-5622; Fax: 310-825-5762; E-mail: pbajaj@mednet.ucla.edu.

[4] The abbreviations used are: TFPI-1, tissue factor pathway inhibitor type 1; TFPI-2, tissue factor pathway inhibitor type 2; pKLK, plasma kallikrein; FXIa, factor XIa; FVIIa, factor VIIa; FXa, factor Xa; FV, factor V; TF, tissue factor; tPA, tissue-type plasminogen activator; uPA, urokinase-type plasminogen activator; KD1-WT, wild-type Kunitz domain 1 of TFPI-2; ECM, extra cellular matrix; pdFV, plasma-derived FV; rFVa, recombinant FVa; PMA, phorbol 12-myristate 13-acetate; TRAP, thrombin receptor activation peptide; rTF, recombinant TF; PL, phospholipid; TFPI-1_{161}, TFPI-1 containing residues 1–161; PRP, platelet-rich plasma; PPP, platelet-poor plasma; SPR, surface plasmon resonance; BR, basic region; AR, acidic region.

tor(s) present on macrophages, smooth muscle cells, endothelial and epithelial cells, keratinocytes, and fibroblasts (16–18). Further, invasive properties of tumor cells are dependent upon the cell surface expression of plasminogen receptors as well as plasmin-mediated proteolysis of ECM (18–22). Importantly, cells that express plasminogen and uPA receptors also express TFPI-2. In this context, keratinocytes (23), dermal fibroblasts (23), smooth muscle cells (7), ciliary epithelium (24), syncytiotrophoblasts (25), synovioblasts (26), and endothelial cells (6) synthesize and secrete TFPI-2 into the ECM. Three variants of molecular mass ~27, ~31, and ~33 kDa are synthesized by these cells and represent differentially glycosylated forms (4, 6). Taken together, the secretion of TFPI-2 into the extravascular space regulates ECM turnover and tumor invasion (9, 27–29) by a mechanism that involves its inhibitory activity toward plasmin (30).

In addition to regulating ECM turnover, TFPI-2 could potentially play an important role in the inhibition of pKLK and FXIa as well as tPA-induced clot fibrinolysis. Human plasma TFPI-2 levels are reported to be negligible (6, 31–36); however, a mean value of 30 pM (range from 3 to 300 pM) in one study (37) and an average value of 0.5 nM (range not given) in an another study (38) have also been reported. Thus, plasma levels of TFPI-2 are below the limit of detection (≤20 pM or 0.5 ng/ml) in the majority of the reports and are also observed to be low in the TFPI-2-transfected apoE-knock-out mice (39). These observations suggest that the plasma concentration of TFPI-2 is too low to impact hemostasis or fibrinolysis. Nevertheless, during hemostasis, platelets play a significant role in producing a localized platelet/fibrin plug to stop the blood loss; this is followed by containment, stabilization, and dissolution of the clot (40, 41). Accordingly, if the platelets contain TFPI-2, its release at the injury site could supplement the known clotting (42, 43) and fibrinolytic inhibitors (44) and provide support in limiting the clot size and its stabilization. To date, neither the expression of TFPI-2 by megakaryocytes nor its presence in platelets has been evaluated.

Interestingly, plasma TFPI-2 levels rise steadily during normal pregnancy and are highest at the onset of labor (31–36). The plasma TFPI-2 levels in the third trimester of pregnancy range from the early reports of 1–3 nM (31–35) to up to 10 nM in recent reports (36, 38). In one study, the mean plasma TFPI-2 level in pregnancy is reported to be 320 pM (31). However, this represents an average value from the beginning of pregnancy to an unspecified gestation period; thus, this value does not reflect the true level of TFPI-2 at the onset of labor. TFPI-2 is abundantly made by syncytiotrophoblasts during pregnancy (45); its role could be to supplement inhibition of fibrinolysis to control bleeding. Noticeably, TFPI-1 is associated with FV in normal plasma (46, 47) and binds to purified FV (46) and FVa (47). Currently, association of TFPI-2 with purified FV or FV in plasma of pregnant women is not known; further, contribution of plasma TFPI-2 toward the inhibition of intrinsic coagulation and/or fibrinolysis has not been determined.

Human FV is a 330-kDa single-chain glycoprotein organized into domain structure A1-A2-B-A3-C1-C2 (42, 48, 49). The second and third A domains are separated by a large heavily glycosylated B-domain, consisting of 836 amino acids located between residues 709 and 1546 of FV. Prior to participation in the coagulation cascade, FV is activated to FVa by proteolysis at Arg-709, Arg-1018, and Arg-1545 with concomitant release of the B-domain in two fragments (amino acids 710–1018 and 1019–1545). Although FXa can activate FV, thrombin is the most robust activator of FV (48). Compared with thrombin, FXa preferentially cleaves at Arg-1018 and Arg-709, yielding an intermediate that has partial FVa activity (50); in this case, only residues 710–1018 of the B-domain are released. Subsequently, FXa slowly cleaves at Arg-1545 to yield the fully active FVa molecule (50, 51). Recent evidence indicates that the release of the B-domain from FV is not a prerequisite for development of FVa activity (52, 53). The B-domain contains two highly conserved sequences, termed the basic region (BR, residues 963–1008) and the acidic region (AR, residues 1493–1537). The BR and the AR interact with each other and maintain FV in its inactive state (52, 53). Removal of either the BR or the AR results in a constitutively active FVa molecule, and removal of both regions yields the fully active FVa molecule (52, 53). Further, similar to the BR of FV, the C-terminal regions of TFPI-1 and TFPI-2 contain several Arg and Lys residues (1–3). This basic C-terminal region of TFPI-1 plays an important role in binding to FV/FVa (47, 54–56). However, the potential role of the TFPI-2 C-terminal basic region in binding to FV/FVa is not known.

In this report, we used RT-PCR, Western blotting, immunohistochemistry, and confocal microscopy to assess the expression of TFPI-2 by a megakaryoblastic cell line (MEG-01), platelets, and bone marrow megakaryocytes. In further studies, we examined binding of TFPI-2 to plasma-derived FV (pdFV), partially B-domain-deleted FV (FV-1033)[5] (57), and recombinant FVa (rFVa); these data were then compared with the data obtained using TFPI-1. We also examined whether TFPI-2 binds to FV in the plasma of pregnant women and whether or not platelets contain TFPI-2 that is associated with FV/Va. Finally, the anticoagulant and antifibrinolytic role of TFPI-2 in platelets and in plasma from women at the onset of labor was assessed.

EXPERIMENTAL PROCEDURES

Reagents—Q-Sepharose FF, Superdex 200, and His-Trap HP columns were obtained from Amersham Biosciences, and normal pooled plasma was obtained from George King Bio-Medical Inc. Thromboplastin reagent (Neoplastin) and rabbit anti-plasmin antibody were purchased from Diagnostic Stago. Alteplase (tPA) was purchased from Genentech, and FXIa was obtained from Enzyme Research Laboratories. Plasmin, pKLK, immunodepleted FV-deficient plasma, mouse monoclonal anti-TFPI-1 N-terminal antibody, anti-human FV-light chain monoclonal antibody resin (AHV-5101-Seph), and sheep anti-human FV polyclonal antibody were obtained from Hemato-

[5] FV-1033 is recombinant FV in which B-domain residues 1034–1491 have been deleted. It contains both the basic (963–1008; FV-BR) and the acidic residues (1492–1538; FV-AR) of the B-domain of FV. Thus, FV-1033 is equivalent to pdFV in all biological properties investigated (57). TFPI-1_{BR} refers to residues 240–265 of TFPI-1, and TFPI-2_{BR} refers to residues 187–213 of TFPI-2. FV_{AR} and FVa_{AR} represent molecules that lack the FV-BR region but contain the FV-AR region. In platelet FVa_{AR}, the peptide bond between Arg-1545 and Ser-1546 is not cleaved (50). FVa_{AR} can be obtained either by limited proteolysis by FXa or by mutating Arg-1545 to Gln in FV (56).

logic Technologies. Phosphatidylserine and phosphatidylcholine were obtained from Avanti Polar Lipids. Restore Western blot stripping buffer and SuperSignal West Femto maximum sensitivity substrate kit were obtained from Thermo Scientific. Phorbol 12-myristate 13-acetate (PMA), polyethylene glycol (PEG) 8000, apyrase, benzamidine, *o*-phenylenediamine dihydrochloride, Ficoll Paque Plus, donkey anti-sheep IgG-HRP (horseradish peroxidase), goat anti-rabbit IgG-HRP, rabbit anti-mouse IgG-HRP, thrombin receptor activation peptide (TRAP), and bovine serum albumin (BSA) were from Sigma. FXIa and pKLK substrate S-2366 (pyro-Glu-Pro-Arg-*p*-nitroanilide) and the plasmin substrate S-2251 (H-D-Val-Leu-Lys-*p*-nitroanalide) were from Diapharma. The mouse IgG isotype and mouse monoclonal antibodies to human CD41a (αIIbβ3), CD45 (leukocyte common antigen), and CD235a (glycophorin A) used for flow cytometry were from BD Biosciences. Alexa Fluor 488 goat anti-rabbit IgG and Alexa Fluor 594 goat anti-mouse IgG were from Invitrogen. The mouse anti-human CD41 antibody used in immunofluorescence experiments was from One World Lab. The rabbit anti-TFPI-2-specific antibody (6) and the murine monoclonal anti-TFPI-2 SK9 antibody (30) were received from Dr. Kisiel, and the bacterial TFPI-2 expression clone (58) was obtained from Dr. Rao. Rabbit polyclonal anti-TFPI-1 C-terminal antibody was received from Dr. Broze (59). SK9 monoclonal antibody was coupled to CNBr-activated Sepharose at 1 mg/ml settled resin using the protocol outlined by GE Healthcare.

Proteins—TFPI-2 and KD1-WT were expressed and purified as described earlier (11, 12, 58). FV-1033, pdFV, and rFVa were obtained as described (57). Recombinant tissue factor (rTF) containing the transmembrane domain (residues 1–243) was reconstituted into phospholipid (PL) vesicles as outlined (60). Full-length TFPI-1 and TFPI-1_{161} (TFPI-1 containing residues 1–161) were provided by Novo Nordisk.

Protease Inhibition Assay—FXIa (1 nM), pKLK (1 nM), or plasmin (3 nM) was incubated with various concentrations of TFPI-2 or KD1-WT for 1 h at room temperature in a 96-well microtitration plate (total volume, 100 μl) as outlined (11, 12). The buffer used was 50 mM Tris-HCl, 100 mM NaCl, pH 7.4 (TBS, pH 7.4) containing 0.1 mg/ml BSA (TBS/BSA) and 2 mM Ca^{2+}. Briefly, 5 μl of synthetic substrate, S-2251 for plasmin and S-2366 for FXIa and pKLK, was then added (final concentration, 1 K_m), and residual amidolytic activity was measured in a Molecular Devices V_{max} kinetic microplate reader. The inhibition constants (K_i*) were determined using the non-linear regression data analysis program Grafit. Data were analyzed with an equation for a tightly binding inhibitor (Equation 1), where v_i and v_0 are the inhibited and uninhibited rates, respectively, and $[I]_0$ and $[E]_0$ are the total concentrations of inhibitor and enzyme, respectively (61, 62).

$$v_i = v_0 \frac{((K_i^* + [I]_0 + [E]_0)^2 - 4[I]_0[E]_0)^{1/2} - (K_i + [I]_0 - [E]_0)}{2[E]_0} \quad \text{(Eq. 1)}$$

K_i values were obtained by correcting for the effect of synthetic substrate concentration, as outlined by Beith (61), using Equation 2, where [S] is substrate concentration, and K_m is specific for each enzyme.

$$K_i = \frac{K_i}{(1 + [S]/K_m)} \quad \text{(Eq. 2)}$$

Blood Collection and Platelet Preparation—Protocols for human studies were approved by the UCLA institutional review board, and informed consent was obtained from all participants. Platelets were isolated as described (63). Fifty ml of blood was collected from normal subjects into acid citrate dextrose anticoagulant (12 mM trisodium citrate·$2H_2O$, 10 mM citric acid monohydrate, and 15 mM dextrose) and centrifuged at 200 × *g* at room temperature for 20 min. Apyrase (final concentration, 0.25 unit/ml) was added to platelet-rich plasma (PRP) and incubated for 10 min at 37 °C prior to centrifugation at 800 × *g* for 20 min at room temperature. Platelet-poor plasma (PPP) was centrifuged again at 800 × *g* to remove traces of platelets. The platelet pellet was resuspended in 10 ml of 15 mM HEPES-buffered Tyrode's solution (0.13 M NaCl, 5 mM KCl, and 6 mM dextrose, pH 6.5) containing 2 mg/ml BSA and 0.25 unit/ml apyrase; the suspension was incubated for 10 min at 37 °C and centrifuged at 800 × *g* for 10 min. The platelets were resuspended in 10 ml of the above Tyrode's solution, washed, and suspended in 3 ml of the above buffer without apyrase and counted on a Beckman Coulter counter. Platelets were activated with 10 μM TRAP for 10 min at 37 °C, at which point benzamidine was added to yield 1 mM concentration. The suspension was centrifuged at 12,000 × *g* for 30 min for Western blot and plasmin ligand blot analysis.

Ten ml of citrated blood was obtained from each healthy pregnant woman (5 subjects in total) at the onset of labor. FV (~81–123%) and platelet counts (2.3–3.1 × 10^5/μl) were in the normal range. Fibrinogen levels were 421 ± 92 mg/dl in late pregnancy plasma, which represents an ~200% increase as compared with normal healthy subjects. PPP and platelets were isolated as above for use in plasmin ligand blot and plasma clot fibrinolysis assays. TFPI-2 in normal PPP, in pregnant woman PPP, and in adult platelets was measured by the procedure outlined by Iino *et al.* (6).

Flow Cytometry—To examine whether platelets in the cord blood also contain TFPI-2, the blood was subjected to Ficoll-Paque gradient centrifugation, and the red blood cell-depleted fraction was used to sort for the CD41a-positive fraction containing platelets and to remove leukocytes (CD45) and the contaminating red blood cells (CD235a). After incubation with the appropriate antibodies, cells were washed with phosphate-buffered saline (PBS) containing 1% BSA and analyzed using a BD FACSAria or LSRII cytometer (BD Biosciences). FACS files were exported and analyzed using FACSDiva software (BD Biosciences). The isolated platelets were smeared on a glass slide, fixed with cold methanol, air-dried, and blocked with 2% normal horse serum before incubating with the rabbit anti-TFPI-2 antibody (16 μg/ml in TBS/BSA) overnight at 4 °C. The bound rabbit anti-TFPI-2 was detected using Alexa Fluor 488 (green) anti-rabbit IgG at a 1:100 dilution in TBS/BSA.

Expression of CD41 and TFPI-2 in MEG-01 Cells Using RT-PCR and Western Blotting—MEG-01 human megakaryocyte leukemia cells obtained from American Type Culture Collection were maintained in RPMI 1640 medium with 10% fetal bovine serum (FBS) and 1% penicillin-streptomycin at 37 °C in

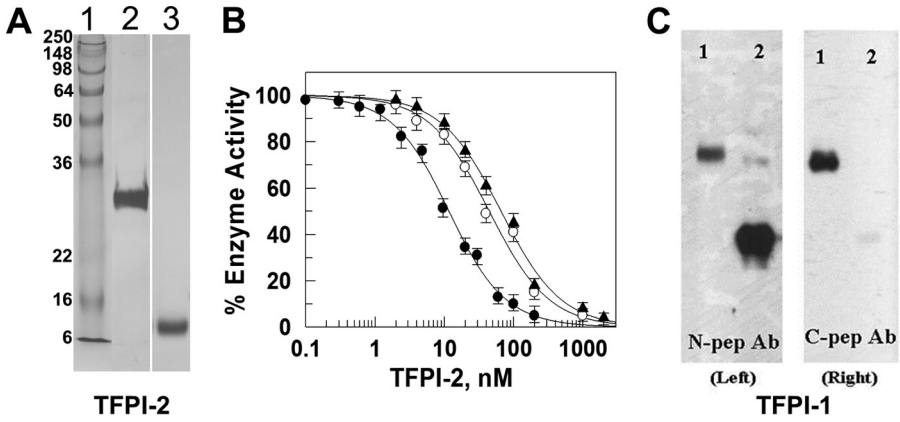

FIGURE 1. **Purification and inhibitory constants (K_i) of TFPI-2 and Western blot analysis of TFPI-1.** *A*, SDS-PAGE analysis of TFPI-2 and KD1-WT. KD1-WT and TFPI-2 were expressed, purified, and refolded as described (11, 58). *Lane 1*, molecular weight markers; *lane 2*, TFPI-2 (M_r ~26,000); *lane 3*, KD1-WT (M_r ~8000). SDS-PAGE was performed using the Laemmli buffer system (68). Acrylamide concentration was 12%, and β-mercaptoethanol was 5% (v/v). *B*, equilibrium inhibition constants (K_i) of TFPI-2 with plasmin, FXIa, and pKLK. The enzyme activity (mean of three experiments) is expressed as the percentage of fractional activity (inhibited/uninhibited) at increasing TFPI-2 concentrations: percentage of activity of 3 nM plasmin (●), percentage of activity of 1 nM FXIa (○), and percentage of activity of 1 nM pKLK (▲). The inhibition constants (K_i) were determined as outlined under "Experimental Procedures." *C*, Western blot analysis of TFPI-1 and TFPI-1_{161}. Reduced samples (10 ng each) were electrophoresed on 12% SDS-PAGE and transferred to nitrocellulose membrane. The primary antibody used was mouse N-terminal TFPI-1 peptide antibody (*left*) or the rabbit C-terminal TFPI-1 peptide antibody (*right*). The secondary antibody used was HRP-conjugated rabbit anti-mouse IgG (*left*) or donkey anti-rabbit IgG (*right*). The protocol used was as outlined by the manufacturer for the mouse monoclonal antibody, and by Broze and co-workers (47, 59) for the rabbit polyclonal antibody. The blots were developed with the SuperSignal Femto chemiluminescent substrate for 5 min and scanned using Alpha Innotech FluorChem FC2 digital imaging system. In both *left* and *right panels*, *lane 1*, full-length TFPI-1; *lane 2*, TFPI-1_{161} that lacks the third Kunitz domain and the C-terminal basic segment.

5% CO_2. For induced expression of CD41 and TFPI-2, the MEG-01 cells were cultured in the presence of 10 ng/ml PMA for 8 days (64, 65). Total RNA was prepared from ~10^6 cells using the RNeasy kit (Qiagen) with DNase I treatment as per the manufacturer's protocol. One μg of RNA in 20 μl was reverse transcribed into cDNA using random primers and the SuperScript III first strand synthesis kit (Invitrogen) containing Moloney murine leukemia virus reverse transcriptase. The cDNA mixture was diluted 1:10, and 1 μl was used for amplification of a 440-bp region of human TFPI-2 using the following primers: forward, 5′-GTCGATTCTGCTGCTTTTCC-3′; reverse, 5′-ATGGAATTTTCTTTGGTGCG-3′ (7). The CD41 expression was analyzed using the following primers: forward, 5′-AGTGCCCCTCGCTGCTCTTTGACC-3′; reverse, 5′-AGTTTTCGGTCTGCCCGGCTCTC-3′ (64). Glyceraldehyde-3-phosphate dehydrogenase (GAPDH) served as a housekeeping gene, using the following primers: forward, 5′-ATCCCATCACCATCTTCCAG-3′; reverse, 5′-CCATCACGCCACAGTTTCC-3′. For TFPI-2 and GAPDH, PCR products were amplified (30 cycles) using 60 °C annealing temperature and 72 °C elongation temperature each for 1 min. For CD41, PCR products were amplified using 58 °C annealing temperature and 72 °C elongation temperature, each for 30 s.

For Western blots (6, 58), the PMA-stimulated and unstimulated MEG-01 cells (2×10^7) were lysed in PBS containing 50 mM octyl-β-D-glucopyranoside, 1 mM phenylmethylsulfonyl fluoride, 10 mg/ml aprotinin, 1 mM sodium orthovanadate, 10 mM EDTA, and 1% Triton X-100 as described (7). After removing the cell debris, protein in each cell lysate was determined using a Bradford protein assay kit; 10 μg was used for 12% SDS-PAGE under nonreducing conditions. The ECM proteins from the cell-free culture plate (150 mm) were eluted with 2 ml of 1% SDS in PBS; 15 μl was used for 12% SDS-PAGE under nonreducing conditions. Proteins were transferred to Bio-Rad PVDF membrane, and Western blot analyses were carried out as detailed for binding of FV to TFPI-2.

Immunofluorescence Staining of MEG-01 Cells—One hundred μl of washed MEG-01 cells (10^5 cells) in cold 1% BSA plus PBS were used to prepare the smears, using 500 rpm for 5 min (Shandon Cytospin 3). The smears were air-dried, permeabilized with ice-cold methanol, and blocked with 2% horse serum for 20 min prior to incubating with rabbit anti-TFPI-2 (16 μg/ml) and mouse anti-CD41 antibody (10 μg/ml) for 2 h at room temperature. After three washes with TBS, 0.05% Tween 20, the slides were incubated with Alexa Fluor 488 (green) anti-rabbit IgG (1:100 dilution), and Alexa Fluor 594 (red) anti-mouse IgG (1:100 dilution) for 30 min in the dark. The slides were washed with TBS plus 0.05% Tween 20, rinsed with deionized water, mounted, and coverslipped using Fluormount-G. Confocal images were obtained using an LSM 700 spinning disk confocal Carl Zeiss microscope with ×63 oil immersion objectives.

Detection of TFPI-2 in Bone Marrow-derived Megakaryocytes—Formalin-fixed paraffin-embedded sections of human fetal bone marrow tissue were used for these studies. The antigen was retrieved by immersing the tissue sections at 60 °C for 30 min in citrate buffer, pH 6.0. The endogenous peroxidase activity was blocked by incubating the sections with 3% H_2O_2 for 10 min. Slides were then incubated with 2% normal horse serum to prevent nonspecific binding. After incubation with rabbit anti-TFPI-2 IgG (16 μg/ml) overnight at 4 °C, the sections were washed (3 times) for 3 min each with PBS plus 0.05% Tween 20 and rinsed with PBS. The sections were then incubated with secondary antibody (goat anti-rabbit IgG-HRP, 1:500 dilution) for 30 min. 3,3′-diaminobenzidine tetrahydrochloride-H_2O_2 substrate was added, and the slides were incubated at room temperature for 3 min. Specimens were counterstained lightly with hematoxylin. Slides were dehydrated and

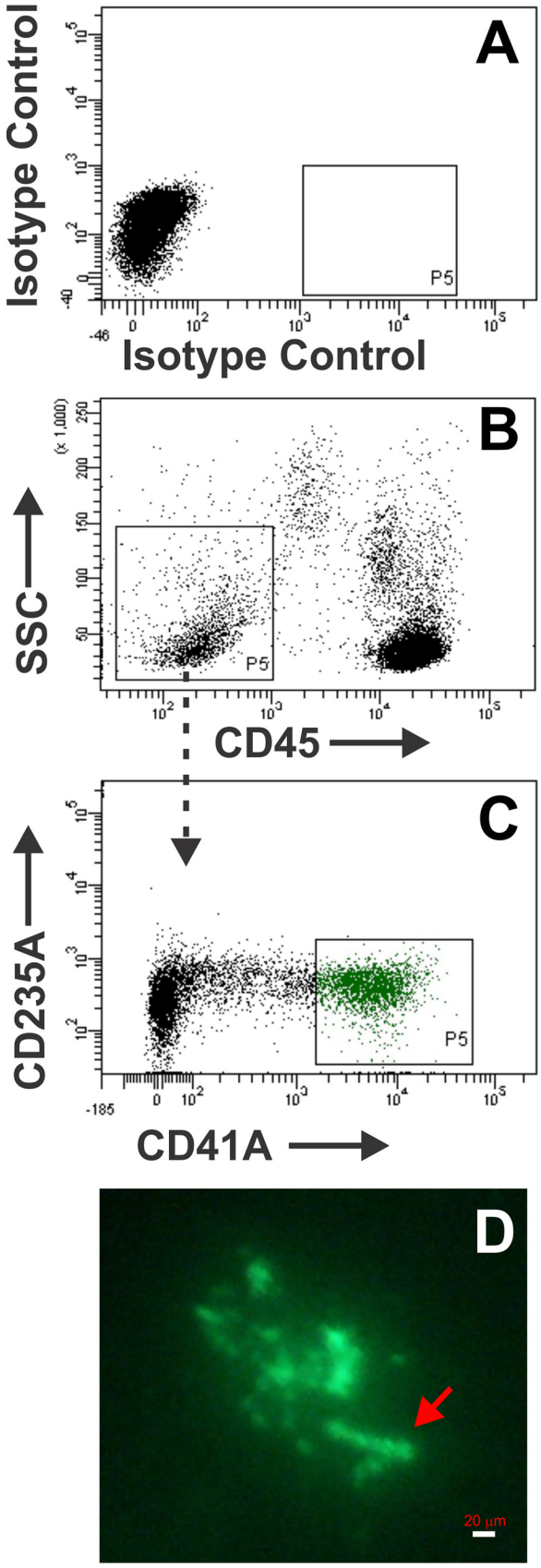

FIGURE 2. **Flow cytometry and fluorescence microscopy to detect TFPI-2 in cord blood platelets.** *A*, dot plot analysis of red blood cell-depleted cord blood cells using the fluorescent labeled mouse isotype IgG. *B*, gating of red blood cell-depleted cord blood cells stained for allophycocyanin anti-CD45. *C*, dot plot analysis of the CD45 negative cells stained for FITC anti-CD235A (glycophorin A) and for the R-phycoerythrin anti-CD41a. *D*, detection of TFPI-2 in platelets by fluorescence microscopy. The anti-CD41a-positive cells sorted using flow cytometry were smeared on a glass slide and stained with rabbit anti-TFPI-2 IgG. The rabbit anti-TFPI-2 IgG was detected using Alexa Fluor 488 (*green*) goat anti-rabbit IgG as described under "Experimental Procedures."

sealed with mounting medium. Images were acquired using the Zeiss Axiovision software version 4.8 Carl Zeiss microscope equipped with ApoTome.2 (modules for Axio Imager.2 and Axio Observer with ×10, ×20, and ×40 (1.3 numerical aperture) and ×63 (1.4 numerical aperture) oil immersion objectives).

TFPI-2 Binding to pdFV, FV-1033, and rFVa—The binding of TFPI-2 or KD1-WT to pdFV, FV-1033, and rFVa was studied using a solid phase protein-binding ELISA technique (66). The Immulon 4HBX microtiter 96-well plates were coated overnight at 4 °C with 100 μl of TFPI-2 or KD1-WT at 10 μg/ml in 50 mM $NaHCO_3$, pH 9.5. The control (background) wells were coated with BSA. The unbound protein was removed by washing the wells three times for 3 min with a washing buffer (25 mM HEPES, 100 mM NaCl, 2 mM $CaCl_2$, pH 7.4, containing 0.1% Tween 20) and blocked for 2 h at room temperature with 300 μl of blocking buffer (25 mM HEPES, 100 mM NaCl, 2 mM Ca^{2+}, pH 7.4, containing 5% nonfat milk). The wells were washed three times with the washing buffer. The pdFV, FV-1033, or rFVa was added to the wells with different concentrations in blocking buffer (100 μl) for 4 h at room temperature. The wells were rinsed (3 times for 5 min each) with the washing buffer and incubated with sheep anti-FV (primary antibody) at 20 μg/ml for 2 h. After washing (3 times for 5 min each), the wells were incubated with donkey anti-sheep IgG-HRP (secondary antibody) at 1:2000 dilution for 1 h. After washing, the bound pdFV or FV-1033 or rFVa was detected using SIGMAFAST™ *o*-phenylenediamine dihydrochloride as substrate for 30 min. The results presented are the average of three determinations.

TFPI-2 and TFPI-1 Binding to FV-1033 and rFVa Using Surface Plasmon Resonance (SPR)—Binding of FV-1033 and rFVa to TFPI-2 and TFPI-1 was also studied using a Biacore T100 flow biosensor (Biacore, Uppsala, Sweden). TFPI-2 or TFPI-1 was immobilized on a carboxymethyl-dextran flow cell (CM5 sensor chips, GE Healthcare) using amine-coupling chemistry. Flow cell surfaces were activated with a mixture of 1-ethyl-3-(3-dimethylaminopropyl) carbodiimide and *N*-hydroxysulfosuccinimide for 5 min at 10 μl/min, after which TFPI-2 or TFPI-1 in 10 mM sodium acetate, pH 5.5, was injected across the flow cell. Unreacted sites were blocked with 1 M ethanolamine. Each analyte (FV-1033 and rFVa) was perfused (10 μl/min) through flow cells in HBS-P buffer (20 mM HEPES, 100 mM NaCl, 2 mM Ca^{2+}, pH 7.4, 0.01% P20, 0.1% PEG 8000). Four-min association and 10-min dissociation times were used. Flow cells were regenerated with HBS-P containing 1 M NaCl followed by equilibration with HBS-P buffer. Data were corrected for nonspecific binding by subtracting the signal obtained with the analyte infused through a flow cell without the coupled protein. Dissociation constants (K_d) were obtained using the equilibrium response (RU_{eq}) for each concentration of FV-1033 or rFVa. Data were fitted to the steady-state 1:1 interaction

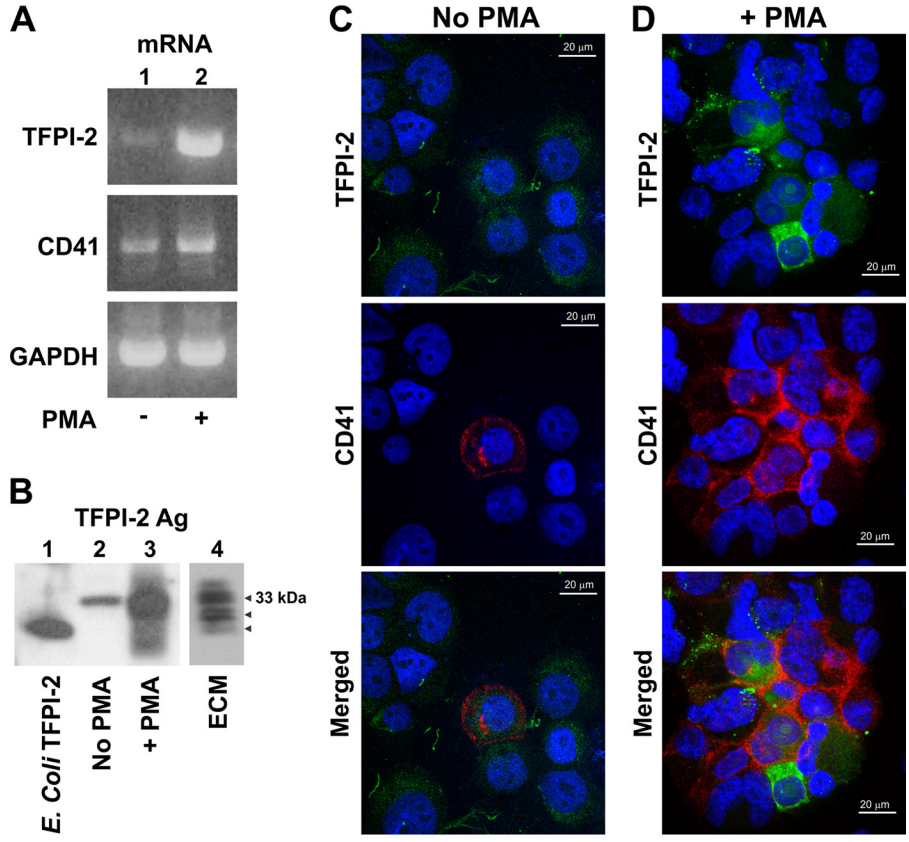

FIGURE 3. **Expression of TFPI-2 and CD41 by MEG-01 cells.** *A*, RT-PCR detection of TFPI-2 and CD41 transcripts in mRNA extracted from MEG-01 cells. Equal amounts of mRNA were reverse transcribed, PCR-amplified, and analyzed by agarose gel electrophoresis. GAPDH served as the housekeeping gene. Shown are unstimulated (*lane 1*) and PMA-stimulated MEG-01 cells (*lane 2*). *B*, Western blot analysis of TFPI-2 and CD41 expression by MEG-01 cells before and after stimulation with PMA. *Lane 1*, 100 ng of TFPI-2; *lane 2*, unstimulated cell lysate (10 μg); *lane 3*, PMA-stimulated cell lysate (10 μg); *lane 4*, ECM from PMA-stimulated cells (15 μl of 2 ml 1% SDS from a 150-mm culture plate). The *arrows* indicate differently glycosylated TFPI-2 species. *C*, confocal microscopy of unstimulated MEG-01 cells depicting the expression of TFPI-2 (*green*) and CD41 (*red*). *D*, confocal microscopy of PMA-stimulated MEG-01 cells depicting increased expression of TFPI-2 (*green*) and CD41 (*red*). The *merged images* in *C* and *D* reveal that CD41 is membrane-associated, and TFPI-2 is intracellular.

equation, $RU_{eq} = (RU_{max} \times C)/(K_d + C)$, where C represents the concentration of FV-1033 or rFVa, and RU_{max} is the maximum binding capacity. The dissociation constants (K_d) were obtained using the non-linear regression data analysis program Grafit.

TFPI-2 Binding to pdFV, FV-1033, and rFVa using Pull-down Assay and Western Blots—One hundred μl of pdFV, FV-1033, or rFVa (each at 30 nM) was incubated with 100 μl of purified TFPI-2 (150 nM) in TBS/BSA, pH 7.4, 2 mM calcium, 1 mM benzamidine for 2 h at room temperature. The complex was then incubated with either 100 μl of AHV-5101-Seph resin or with anti-TFPI-2 SK9 antibody resin overnight at 4 °C in the same buffer. The samples were centrifuged, and the resin was washed four times with 0.5 ml of the incubation buffer. The bound complexes were eluted with 40 μl of SDS sample buffer, 6 M urea (50 °C for 30 min) and run on 10% SDS-PAGE under non-reducing conditions. The proteins were transferred to Bio-Rad PVDF membrane and probed overnight with rabbit anti-TFPI-2 antibody (6, 58) at 16 μg/ml in TBS plus 1% nonfat milk. The secondary antibody used was goat anti-rabbit IgG-HRP at 1:15,000 dilution in TBS plus 1% milk for 2 h. The blots were developed with the SuperSignal Femto chemiluminescent substrate for 5 min and scanned using Alpha Innotech FluorChem FC2 digital imaging system. The blots were stripped with Thermo Scientific Restore Western blot stripping buffer and then probed with sheep anti-FV antibody (20 μg/ml in TBS plus 1% milk, overnight). The secondary antibody used was donkey anti-sheep IgG-HRP (1:2000 dilution in TBS plus 1% milk for 2 h), and the blots were developed and scanned similarly.

Association of TFPI-2 with FV in Plasma of Pregnant Women and in Normal Platelets—One ml of plasma from each pregnant woman and their pooled plasma as well as 1 ml of normal pooled plasma were incubated (in the absence of Ca^{2+}) with either anti-FV AHV-5101-Seph resin or with anti-TFPI-2 SK9 antibody resin as described above. Similarly, the TRAP-activated platelet supernatants from normal individuals and pregnant women were incubated with anti-FV AHV-5101-Seph resin or with anti-TFPI-2 SK9 antibody resin and processed for Western blots as outlined above.

Plasma Clot Fibrinolysis—With slight modification, the procedure used was that described previously (11, 12, 67). FXIa or rTF was used to initiate intrinsic or extrinsic clotting and fibrin formation in plasma. Two hundred twenty-five μl of PPP, PRP containing 3×10^8 platelets/ml, or PPP from pregnant women at the onset of labor were mixed with 12.5 μl of PL vesicles and 12.5 μl of buffer or rabbit anti-TFPI-2 IgG. In experiments where PPP was used, 240 μl of the above mixture was added to

10 μl of FXIa (or rTF) and tPA in TBS/BSA containing 250 mM $CaCl_2$. In the 250-μl final volume, concentration of FXIa was 400 pM (or 10 pM rTF), PL was 100 μM, and tPA was 0.5 μg/ml. In the second set of experiments where PRP was used, 240 μl of the mixture was added to 10 μl of FXIa (or rTF) and tPA in TBS/BSA containing 250 μM TRAP and 250 mM $CaCl_2$. In this case, the 250-μl final volume contained 400 pM FXIa (or 10 pM rTF), 100 μM PL, 0.5 μg/ml tPA, and 10 μM TRAP. The effect of TFPI-2 present in platelets or in pregnant woman plasma was evaluated by including rabbit anti-TFPI-2 IgG at 300 μg/ml in the final 250-μl mixture. In control experiments, non-immune rabbit IgG or anti-TFPI-2 IgG at 300 μg/ml was added to PPP (that lacks TFPI-2) in order to rule out their contributions to the plasma clot lysis. In additional experiments, PPP was supplemented with 7 nM TFPI-2 (comparable with that in pregnant woman PPP) to assess its effect on clotting and/or fibrinolysis. Clot formation and lysis were monitored at 37 °C with a microplate reader (SPECTRAmax 190, Molecular Devices) by measuring the optical density at 405 nm (A_{405}) as described (11, 12).

Plasmin Ligand Blot to Assess TFPI-2 in Platelets—Thirty μl of TRAP-activated platelet suspension (3×10^8 platelets) was centrifuged, and supernatant and the pellet were subjected to 12% SDS-PAGE under nonreducing conditions. Western blot analysis was carried out as above except that plasmin (20 μg/ml) was used as the ligand. The bound plasmin was detected by the rabbit anti-plasmin antibody (1:100 dilution) followed by incubation with goat anti-rabbit IgG-HRP at 1:15,000 dilution.

RESULTS

Characterization of TFPI-2 and TFPI-1—TFPI-2 and KD1-WT were expressed in *Escherichia coli* and purified by previously established procedures (11, 58). Both proteins had the expected molecular weights as determined by SDS-PAGE (Fig. 1*A*). TFPI-2 inhibited plasmin, FXIa, and pKLK with K_i values of 5 ± 1, 19 ± 3, and 31 ± 5 nM, respectively (Fig. 1*B*). KD1-WT inhibited plasmin, FXIa, and pKLK with K_i values of 6 ± 1, 18 ± 2, and 26 ± 3 nM, respectively (data not shown). Our K_i values for TFPI-2 and KD1-WT are in excellent agreement with previously reported K_i values (5, 8, 11, 58) for each protease, suggesting proper folding of the recombinant domains. Further, full-length TFPI-1 reacted with the antibodies to the N-terminal and C-terminal peptides, whereas TFPI-1_{161} reacted with only the antibody to the N-terminal peptide (Fig. 1*C*). These data establish that TFPI-2, KD1-WT, TFPI-1, and TFPI-1_{161} are suitable for FV and FVa binding studies presented later in this report.

TFPI-2 Levels in Plasma and Platelets—TFPI-2 antigen was undetectable (<1 ng/ml or <30 pM) in PPP from healthy subjects ($n = 5$) using the method described by Iino *et al.* (6). TFPI-2 antigen ranged from 5.8 to 8.1 nM (170–252 ng/ml) in five pregnant women at the onset of labor; the pooled plasma contained 7.1 nM TFPI-2. Further, supernatants from 3×10^8 TRAP-activated platelets obtained from normal healthy adults contained 69–95 ng (average ~85 ng) of TFPI-2.

Flow Cytometry and Fluorescence Microscopy to Detect TFPI-2 in Cord Blood Platelets—Next, we examined whether platelets in the cord blood also contain TFPI-2. We used flow cytometry to obtain platelets free of other blood cells. The platelets were stained with rabbit anti-TFPI-2 antibody followed by Alexa Fluor 488 anti-rabbit IgG. The data presented in Fig. 2 clearly reveal that the TFPI-2 antigen is present in the cord blood platelets.

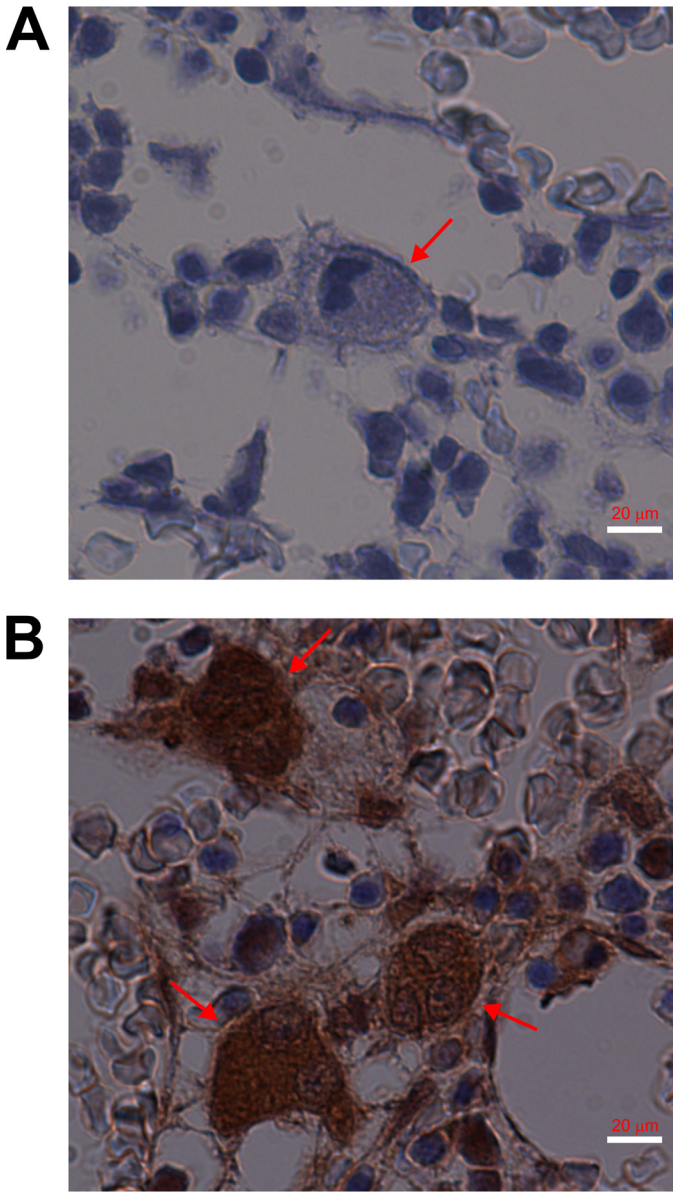

FIGURE 4. **Localization of TFPI-2 antigen in the megakaryocytes of bone marrow.** The formalin-fixed paraffin-embedded sections of the fetal bone marrow tissue were processed as outlined under "Experimental Procedures" and stained with either non-immune rabbit IgG (*A*) or rabbit anti-TFPI-2 IgG (*B*) followed by goat anti-rabbit IgG-HRP. 3,3′-Diaminobenzidine tetrahydrochloride-H_2O_2 was used to detect the bound anti-rabbit IgG-HRP, and hematoxylin was used to stain for RNA/DNA. In both *A* and *B*, *arrows* show the megakaryocytes.

Expression of TFPI-2 and CD41 by MEG-01 Cells and Bone Megakaryocytes—Here, we examined the expression of TFPI-2 and CD41 by the megakaryoblastic MEG-01 cells using RT-PCR (Fig. 3*A*), Western blots (Fig. 3*B*) and immunofluorescence (Fig. 3, *C* and *D*). The unstimulated MEG-01 cells expressed low levels of TFPI-2 and CD41, whereas PMA-stimulated MEG-01 cells expressed increased levels of TFPI-2 and CD41. In addition to the cell lysates, the ECM of

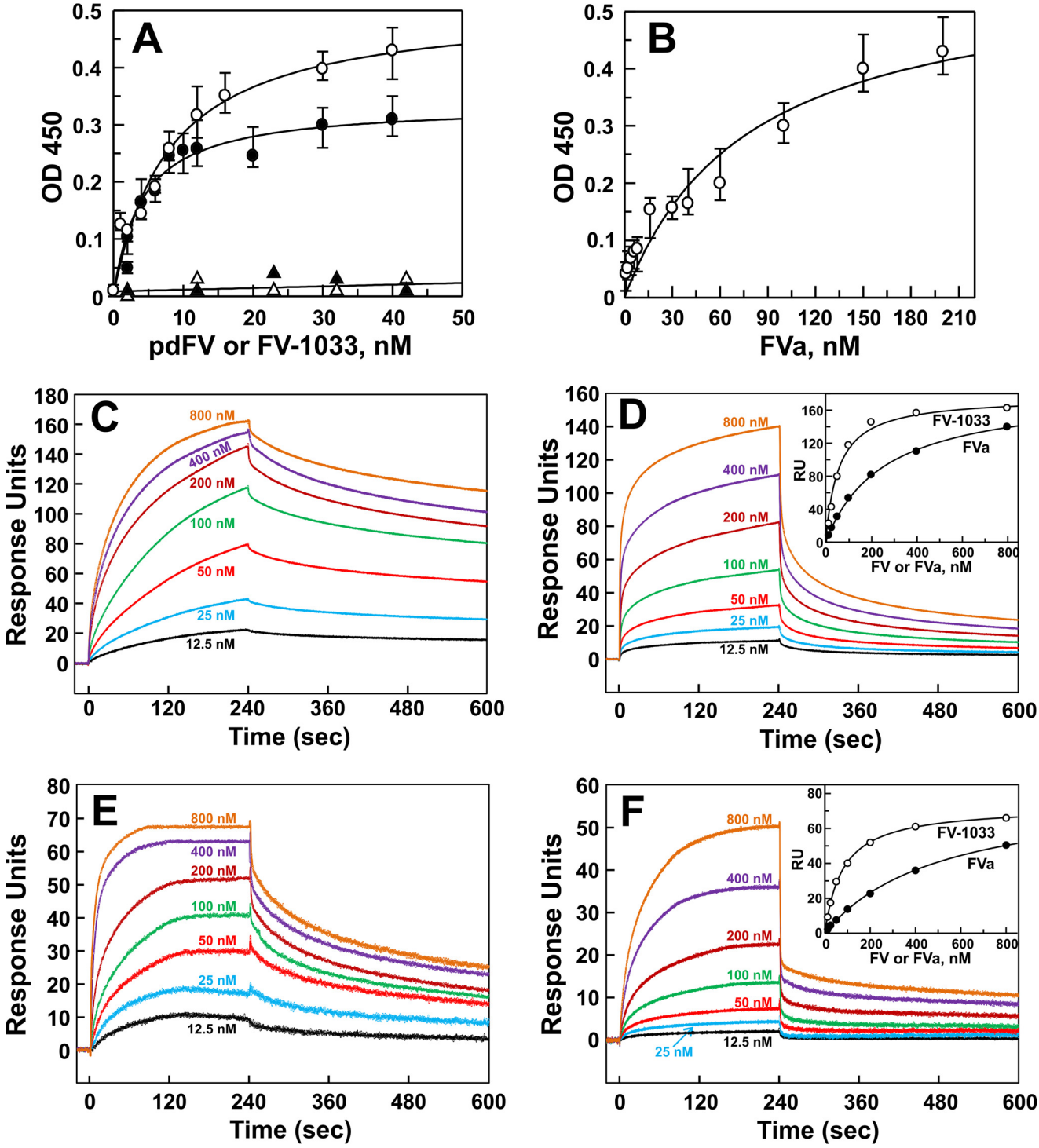

FIGURE 5. **Binding of TFPI-2 and TFPI-1 to FV and FVa.** *A*, binding of pdFV and FV-1033 to immobilized TFPI-2 using ELISA. Shown is TFPI-2 binding to pdFV (●) or FV-1033 (○) and the absence of KD1-WT binding to pdFV (▲) or FV-1033 (△). The protocol used is outlined under "Experimental Procedures." *B*, binding of rFVa to immobilized TFPI-2. The protocol was the same as in *A* except that different concentrations of rFVa were employed. *C*, SPR sensograms of the interaction between FV-1033 and TFPI-2. TFPI-2 was coupled to the CM5 chip by the amine coupling method, and an immobilization level of 658 response units (*RU*) was attained for the bound protein. Seven concentrations (12.5–800 nM) of FV-1033 were used; 4-min association and 10-min dissociation times (flow rate, 10 μl/min) were employed. Details are provided under "Experimental Procedures." *D*, SPR sensograms of the interaction between rFVa and TFPI-2. The TFPI-2-coupled CM5 chip used was the same as in *C*, and seven concentrations (12.5–800 nM) of rFVa were employed. *Inset*, determination of K_d values for the interaction between TFPI-2 and FV-1033 (*open circles*) and between TFPI-2 and FVa (*closed circles*). Response units are plotted against concentration of FV-1033 (*FV*) or rFVa (*FVa*). Details to obtain the K_d values are provided under "Experimental Procedures." *E*, SPR sensograms of the interaction between FV-1033 and TFPI-1. TFPI-1 was coupled to the CM5 chip by the amine-coupling method, and an immobilization level of 624 response units was attained for the bound protein. Seven concentrations (12.5–800 nM) of FV-1033 were used; 4-min association and 10-min dissociation times (flow rate, 10 μl/min) were employed. *F*, SPR sensograms of the interaction between rFVa and TFPI-1. The same TFPI-1-coupled CM5 chip used in *E* above was employed, and seven concentrations (12.5–800 nM) of rFVa were used. *Inset*, determination of K_d values for the interaction between TFPI-1 and FV-1033 (*open circles*, *FV*) and between TFPI-1 and rFVa (*closed circles*, *FVa*).

PMA-stimulated MEG-01 cells also contained significant amounts of TFPI-2 (Fig. 3*B*). The presence of TFPI-2 in the ECM of MEG-01 cells is consistent with the earlier data obtained using ECM from different cell types (6, 23, 27).

In subsequent experiments, we assessed TFPI-2 expression in megakaryocytes using fetal bone marrow tissue. The immunostaining data using non-immune rabbit IgG (Fig. 4*A*) and the rabbit anti-TFPI-2 IgG revealed that the fetal bone megakaryocytes express TFPI-2 (Fig. 4*B*). Cumulatively, the antigen levels in adult platelets and the data presented in Figs. 2–4 support a conclusion that megakaryocytes are the source of platelet TFPI-2.

Binding of TFPI-2 and TFPI-1 to pdFV, FV-1033, and rFVa Using ELISA—Plasma concentration of FV is ~20 nM, and platelets contain ~20% of the total FV present in whole blood (48). Previous work on the association of FV with TFPI-1 raises the possibility that TFPI-2 in platelets and in the plasma of pregnant women might also be associated with FV. We examined the binding of TFPI-2 and KD1-WT to FV and FVa using a solid phase protein-protein interaction assay presented in Fig. 5, *A* and *B*. TFPI-2 bound to pdFV, FV-1033 and rFVa with K_d values of 7 ± 2, 9 ± 3, and 95 ± 11 nM, respectively (Table 1). However, KD1-WT did not bind to pdFV or FV-1033. Moreover, prior incubation (1 h) of 10 nM pdFV or FV-1033 with 100 nM TFPI-1 abrogated ≥90% of their binding to the surface-bound TFPI-2 in the ELISA. However, incubation of pdFV or FV-1033 with TFPI-1_{161} under similar conditions had no effect on their binding to TFPI-2. These data indicate that TFPI-2 and TFPI-1 compete for binding to FV. Moreover, KD1-WT of TFPI-2 or residues 1–161 of TFPI-1 do not significantly contribute to this interaction.

Binding of TFPI-2 and TFPI-1 to FV-1033 and rFVa Using SPR—TFPI-1 has been shown previously to bind to pdFV with ~15 nM K_d using SPR (46). Here, we employed SPR to study the binding of FV-1033 and rFVa to immobilized TFPI-2 or TFPI-1. These data are presented in Fig. 5, *C–F*. The sensograms indicate that the interactions reached equilibrium during the injection of each analyte concentration; therefore, the dissociation constants for TFPI-2 and TFPI-1 with FV-1033 or rFVa could be determined using the relationship between the maximum binding response (RU_{max}) and the analyte concentration (FV-1033 or rFVa) using the steady-state 1:1 interaction equation (see "Experimental Procedures"). TFPI-2 binds to FV-1033 with K_d = 36 ± 4 nM and to rFVa with K_d = 252 ± 16 nM. Similarly, TFPI-1 binds to FV-1033 with K_d = 48 ± 6 nM and to rFVa with K_d =

TABLE 1

Dissociation constants for the binding of TFPI-2 and TFPI-1 to pdFV, FV-1033, and rFVa

In ELISA experiments, TFPI-2 was coated to the Immulon 4HBX microtiter plate. In SPR experiments, TFPI-2 or TFPI-1 was coupled to the CM5 chip. The dissociation constants were obtained using the steady state equilibrium model.

Methodology	Ligand	Analyte	K_d
			nM
ELISA	TFPI-2	pdFV	7 ± 2
	TFPI-2	FV-1033	9 ± 3
	TFPI-2	rFVa	95 ± 11
SPR	TFPI-2	FV-1033	36 ± 4
	TFPI-2	rFVa	252 ± 16
	TFPI-1	FV-1033	48 ± 6
	TFPI-1	rFVa	456 ± 18

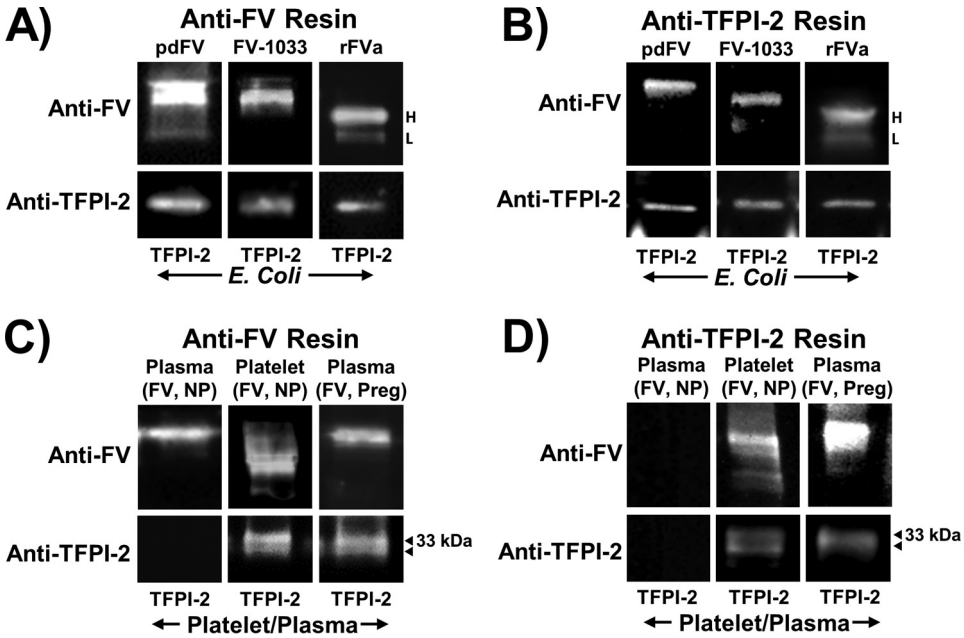

FIGURE 6. **Western blot analysis of TFPI-2 binding to pdFV, FV-1033, and rFVa.** *A* and *B*, Western blots using purified proteins. Each FV species was incubated with *E. coli* expressed TFPI-2 and then with either AHV-5101-Seph resin (*A*) or anti-TFPI-2 SK9 antibody resin (*B*). The bound complexes were eluted, and Western blots were performed using rabbit anti-TFPI-2 antibody and sheep anti-FV antibody as outlined under "Experimental Procedures." The blots were developed with the SuperSignal Femto chemiluminescent substrate and scanned using the Alpha Innotech FluorChem FC2 digital imaging system. The *first* (*left*) *column* in each *panel* shows pdFV/TFPI-2 interaction, the *second column* shows the FV-1033/TFPI-2 interaction, and the *third column* shows rFVa/TFPI-2 interaction. *H*, FVa heavy chain; *L*, FVa light chain. *C* and *D*, Western blot analysis of TFPI-2 binding to plasma FV and platelet FV/Va under *ex vivo* conditions. One ml of normal pooled plasma (*left column* in *C* and *D*), the lysate from 3×10^8 normal platelets (*second column*), or 1 ml of pooled plasma from five pregnant women (similar results were obtained with individual plasma samples) at the onset of labor (*third column*) were incubated with AHV-5101-Seph resin (*C*) or with anti-TFPI-2 SK9 antibody resin (*D*), and the samples were processed for Western blots as in *A* and *B*. The *arrows* indicate differently glycosylated TFPI-2 molecular species (6, 7, 58). Note the presence of several molecular species of FV/Va in the *C* and *D* (*second column*) similar to those observed earlier (56).

456 ± 18 nM. Thus, both TFPI-2 and TFPI-1 bind to FV-1033 with higher affinity than rFVa. These data are summarized in Table 1.

TFPI-2 Binding to pdFV, FV-1033, and rFVa Using Pull-down Assays and Western Blots—The purpose of these experiments was to determine whether TFPI-2 in the plasma of pregnant women and in platelets from normal healthy subjects is associated with FV. For this, we first developed an *in vitro* pull-down assay method followed by Western blots to study this interaction using purified proteins. The data presented in Fig. 6, *A* (using anti-FV AHV-5101-Seph resin) and *B* (using anti-TFPI-2 SK9 antibody resin), confirm that the procedure can be used to study the interaction of TFPI-2 with FV/Va. The data presented in Fig. 6, *C* and *D*, reveal that plasma obtained from women during the onset of labor contained TFPI-2 that, in part, was bound to FV; in contrast, TFPI-2 was not detected in normal plasma. Further, normal platelets also contained TFPI-2 associated with FV/Va (Fig. 6, *C* and *D*).

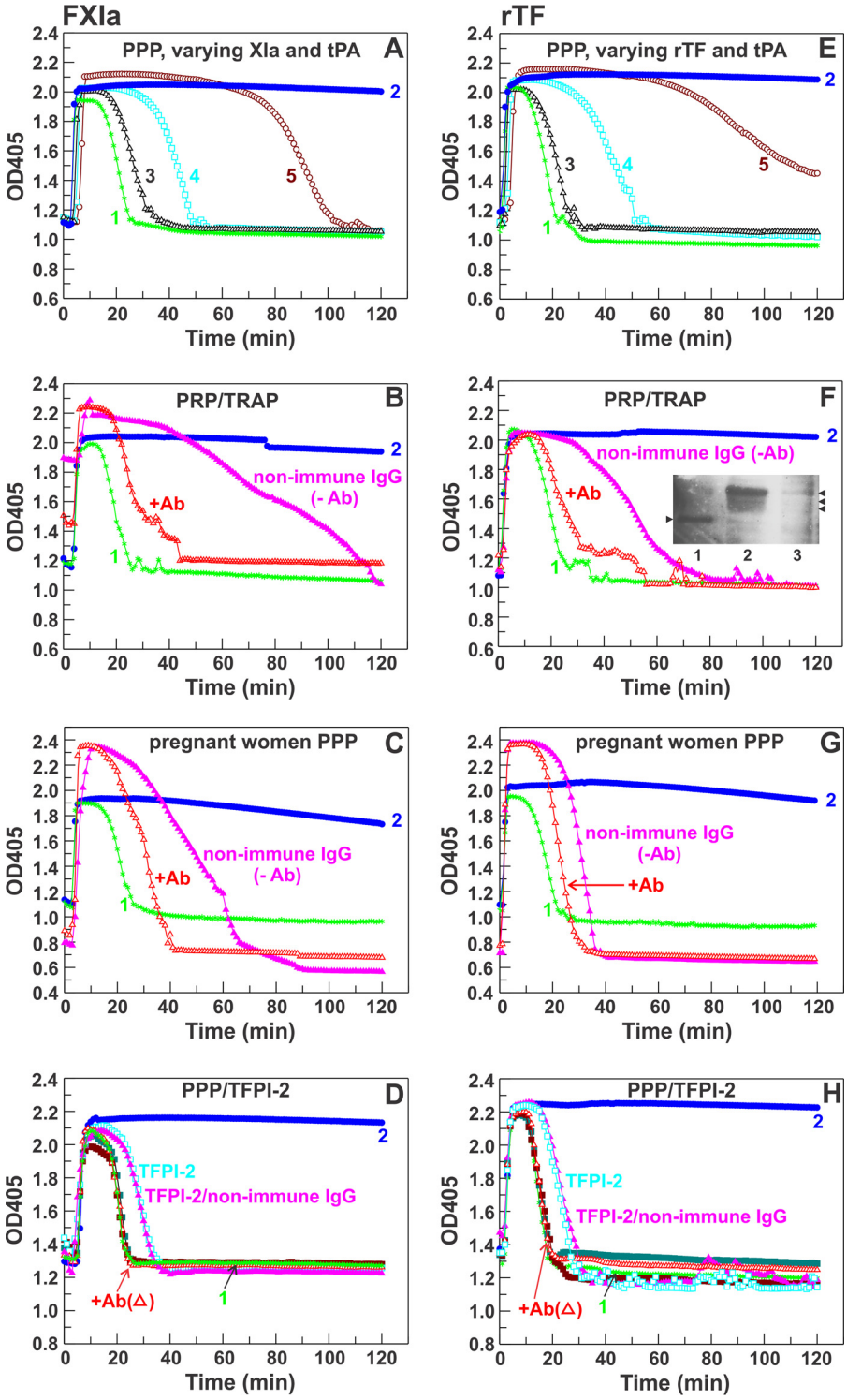

Physiologic Function of TFPI-2 in Platelets and Pregnant Woman PPP—Biologic function of TFPI-2 in normal platelets and in the plasma of pregnant women at the onset of labor was evaluated using intrinsic or extrinsic clotting and tPA-induced fibrinolysis. Initially, the effect of varying concentrations of FXIa and tPA using normal PPP was assessed. These data are shown in Fig. 7*A*. At 400 pM FXIa, 0.5 μg/ml tPA, clot formation started at ~4 min, and complete lysis occurred at ~26 min (*curve 1*); in the absence of tPA, no lysis was evident during the 2-h time course of the experiment (*curve 2*); at 300 pM FXIa, 0.38 μg/ml tPA, the clot formation started at ~5 min, and complete lysis occurred at ~34 min (*curve 3*); at 200 pM FXIa, 0.25 μg/ml tPA, the clot formation started at ~6 min, and complete lysis occurred at ~50 min (*curve 4*); and at 100 pM FXIa, 0.12 μg/ml tPA, the clot formation started at ~7 min, and complete lysis occurred at ~100 min (curve 5). When PPP was replaced by PRP (3×10^8 platelets/ml) at 400 pM FXIa, 0.5 μg/ml tPA, the clot formation started at ~6 min, and complete lysis occurred at ~120 min (Fig. 7*B*, *curve −Ab*). The addition of rabbit anti-TFPI-2 IgG to the PRP reduced the clot formation to ~5 min and lysis to ~42 min (Fig. 7*B*, *curve +Ab*). Thus, by inference, TFPI-2 released from platelets inhibits FXIa by ~25% (in the first 6 min) and tPA-induced lysis by ~50%.

In additional experiments, when normal PPP was replaced by pregnant woman PPP at 400 pM FXIa, 0.5 μg/ml tPA, the clot formation started at ~5 min, and complete lysis occurred at ~80 min (Fig. 7*C*, *curve −Ab*). The addition of rabbit anti-TFPI-2 IgG to the pregnant woman PPP reduced the clot formation to ~4 min and lysis to ~40 min (Fig. 7*C*, *curve +Ab*). Thus, TFPI-2 present in the plasma of pregnant women at the onset of labor inhibits FXIa by ~25% (during the first 5 min) and tPA-induced lysis by ~40%.

To validate the results of Fig. 7, *B* and *C*, we examined the effect of non-immune IgG and anti-TFPI-2 IgG on the clot fibrinolysis of normal PPP; these data presented in Fig. 7*D* reveal no effect, confirming that the anti-TFPI-2 IgG is TFPI-2-specific. Further, when normal PPP was supplemented with 7 nM TFPI-2, it increased the clot lysis time from ~25 min to ~40 min. Moreover, the addition of anti-TFPI-2 IgG reduced the lysis time to ~25 min, similar to PPP (Fig. 7*D*); in contrast, non-immune IgG had no effect.

Next, we assessed the effect of varying concentrations of rTF and tPA while using normal PPP (Fig. 7*E*). At 10 pM rTF, 0.5 μg/ml tPA, the clot formation started at ~2 min, and complete lysis occurred at ~24 min (*curve 1*); in the absence of tPA, no lysis was evident during the 2-h time course of the experiment (*curve 2*); at 7.5 pM rTF, 0.38 μg/ml tPA, the clot formation started at ~3 min, and complete lysis occurred at ~33 min (*curve 3*); at 5 pM rTF, 0.25 μg/ml tPA, the clot formation started at ~4 min, and complete lysis occurred at ~55 min (*curve 4*); and at 2.5 pM rTF, 0.12 μg/ml tPA, the clot formation started at ~5 min, and complete lysis occurred at >120 min (*curve 5*). When PPP was replaced by PRP (3×10^8 platelets/ml) at 10 pM rTF, 0.5 μg/ml tPA, the clot formation started at ~3 min, and complete lysis occurred at ~80 min (Fig. 7*F*, *curve −Ab*). The addition of rabbit anti-TFPI-2 IgG to the PRP did not affect the clot formation time (~3 min) but reduced the lysis time to ~40 min (Fig. 7*F*, *curve +Ab*). Thus, TFPI-2 in PRP inhibits tPA-induced lysis by ~40% but does not affect extrinsic coagulation.

In further experiments, when normal PPP was replaced by PPP from pregnant women at 10 pM rTF, 0.5 μg/ml tPA, the clot formation started at ~2 min, and complete lysis occurred at ~40 min (Fig. 7*G*, *curve −Ab*). The addition of rabbit anti-TFPI-2 IgG to the pregnant woman PPP did not affect the clot formation time but reduced the lysis time to ~30 min (Fig. 7*G*, *curve +Ab*). Thus, TFPI-2 present in the plasma of pregnant women at the onset of labor inhibits tPA-induced lysis by ~30% without affecting extrinsic coagulation. Similar to the results obtained in Fig. 7*D*, non-immune IgG or anti-TFPI-2 IgG had no effect on the clot fibrinolysis of normal PPP when the clotting was initiated with rTF (Fig. 7*H*). In this system, when normal PPP was supplemented with 7 nM TFPI-2, it increased the lysis time from ~24 min to ~36 min. In addition, anti-TFPI-2 IgG reduced the lysis time to a value similar that of PPP (Fig. 7*H*), whereas non-immune IgG had no effect.

Although absolute concentration of TFPI-2 in the PRP was only ~40% of that present in the pregnant woman PPP, the FXIa or plasmin inhibition was more pronounced in the PRP system (Fig. 7, *B versus C* and *F versus G*). A possible explanation for this observation might be that the TFPI-2 in PRP *versus* the pregnant woman PPP is more effectively localized at the

FIGURE 7. **Effect of TFPI-2 in normal PRP and in the pregnant woman PPP on clotting and fibrinolysis.** Clot formation was initiated with FXIa or rTF, and fibrinolysis was induced by the simultaneous addition of tPA. Fibrin formation and lysis were monitored by measuring the optical density at 405 nm as outlined under "Experimental Procedures." *A*, effect of varying FXIa and tPA on clotting and fibrinolysis using normal PPP. *Curve 1*, 400 pM FXIa, 0.5 μg/ml tPA; *curve 2*, 400 pM FXIa, no tPA; *curve 3*, 300 pM FXIa, 0.38 μg/ml tPA; *curve 4*, 200 pM FXIa, 0.25 μg/ml tPA; *curve 5*, 100 pM FXIa, 0.12 μg/ml tPA. *B*, effect of TFPI-2 in PRP/TRAP on intrinsic clotting and fibrinolysis. *C*, effect of TFPI-2 in pregnant woman PPP on intrinsic clotting and fibrinolysis. In *B* and *C*, FXIa was 400 pM and tPA was 0.5 μg/ml, and the *curve labeled −Ab* contained non-immune rabbit IgG, and the *curve labeled +Ab* contained rabbit anti-TFPI-2 IgG. *Control curves 1* and *2* in *B* and *C* represent repeats of *curves 1* and *2* in *A*. Further, anti-TFPI-2 IgG or non-immune rabbit IgG had no effect on clotting or fibrinolysis (see below). *D*, effect of TFPI-2 added to PPP on intrinsic clotting and fibrinolysis. *Control curves 1* (*green*) and *2* (*blue*) are duplicates of *curves 1* and *2* in *A*. Additional components included in the *green curve* are non-immune IgG (*dark green squares*), anti-TFPI-2 IgG (*brown squares*), TFPI-2 (*cyan squares*), and TFPI-2 plus anti-TFPI-2 IgG (*red open triangles*) or plus non-immune IgG (*magenta closed triangles*). TFPI-2 concentration was 7 nM, and non-immune or anti-TFPI-2 IgG was 300 μg/ml. *E*, effect of varying rTF and tPA on clotting and fibrinolysis using normal PPP. *Curve 1*, 10 pM rTF, 0.5 μg/ml tPA; *curve 2*, 10 pM rTF, no tPA; *curve 3*, 7.5 pM rTF, 0.38 μg/ml tPA; *curve 4*, 5 pM rTF, 0.25 μg/ml tPA; *curve 5*, 2.5 pM rTF, 0.12 μg/ml tPA. *F*, effect of TFPI-2 in PRP/TRAP on extrinsic clotting and fibrinolysis. *G*, effect of TFPI-2 in pregnant woman PPP on extrinsic clotting and fibrinolysis. In both *F* and *G*, rTF was 10 pM, and tPA was 0.5 μg/ml, and the *curve labeled −Ab* contained non-immune rabbit IgG, and the *curve labeled +Ab* contained rabbit anti-TFPI-2 IgG. *Control curves 1* and *2* in *F* and *G* represent repeats of *curves 1* and *2* in *E*. *Inset* in *F*, the plasmin ligand blot of TRAP-activated 3×10^8 platelets. *Lane 1*, 50 ng of *E. coli* TFPI-2 (26 kDa); *lane 2*, platelet releasate; *lane 3*, insoluble pellet. The *arrows* indicate differently glycosylated species of TFPI-2 ranging from 27 to 33 kDa. *H*, effect of TFPI-2 added to PPP on extrinsic clotting and fibrinolysis. *Control curves 1* (*green*) and *2* (*blue*) are duplicates of *curves 1* and *2* in *E*. Additional components included in the *green curve* are non-immune IgG (*dark green squares*), anti-TFPI-2 IgG (*brown squares*), TFPI-2 (*cyan squares*), and TFPI-2 plus anti-TFPI-2 IgG (*red open triangles*) or plus non-immune IgG (*magenta closed triangles*). TFPI-2 concentration was 7 nM, and non-immune or anti-TFPI-2 IgG was 300 μg/ml.

platelet aggregation/clot site. Further detailed prospective experiments are needed to address this issue.

Because a major effect of the activated platelets in PRP appears to be the inhibition of tPA-induced fibrinolysis (Fig. 7, *B* and *F*), we examined whether TFPI-2, in part, stays associated with the platelet membrane or is fully released into the medium. To assess this, we activated the isolated platelets from normal subjects and from pregnant woman blood with TRAP and performed plasmin ligand blot analysis. The data for normal platelets are shown in Fig. 7*F* (*inset*). Similar results were obtained with platelets from pregnant subjects (data not shown). Clearly, a majority of the TFPI-2 is released into the medium upon activation of platelets with TRAP.

DISCUSSION

The role of TFPI-2 in regulating ECM turnover and tumor invasion has been well documented and reviewed (8, 9, 27, 30). However, whether or not TFPI-2 plays a role in regulating blood coagulation and/or fibrinolysis remains uncertain. An important reason for this prevailing perspective is the finding (6, 31–36) (present study) that levels of TFPI-2 are undetectable ($\leq$20 pM) in normal plasma. Here, we show that normal platelets, which constitute an integral part of the hemostatic system, contain TFPI-2. TRAP activation of 3×10^8 platelets (average number present per ml of blood) released ~85 ng of TFPI-2, most of which would be localized at the platelet aggregation site. Further, because most of the TFPI-2 is released into the medium (Fig. 7*F*, *inset*), it may be stored in the platelet α-granules. However, additional work will be required to corroborate this view because TFPI-1, a homologue of TFPI-2, has not been localized to α-granules or lysosomes (69).

We suggest that platelet TFPI-2 is derived from megakaryocytes. Three lines of evidence support this possibility. First, TFPI-2 concentration in blood is too low for manifestation of endocytosis by platelets. Second, MEG-01 cells express both TFPI-2 and CD41, as revealed by RT-PCR, Western blotting, and immunofluorescence (Fig. 3). Moreover, PMA up-regulates the expression of CD41 and production of platelets in MEG-01 cells (64, 65). Therefore, PMA-treated MEG-01 cells might also express proportionately increased TFPI-2 for adequate amounts to exist in platelets. Our data presented in Fig. 3 corroborate this conclusion. Finally, the fetal bone marrow tissue stained with rabbit anti-TFPI-2 IgG show the presence of TFPI-2 in megakaryocytes (Fig. 4). Although in our study we used fetal bone marrow tissue, we postulate that adult megakaryocytes would also express TFPI-2. This conclusion is supported by the observation that platelets in the adult (Figs. 6, *C* and *D*, and 7*F* (*inset*)) and in the cord blood (Fig. 2*D*) contain TFPI-2.

In agreement with recent observations (36, 38), our data indicate that plasma levels of TFPI-2 in pregnancy during the onset of labor are ~7 nM. Based upon previous work with TFPI-1 (46, 47, 54–56), we evaluated the binding of TFPI-2 to purified FV and FVa as well as to FV/Va in platelets and FV in pregnant woman plasma. In ELISA experiments, TFPI-2 bound to pdFV and FV-1033 with ~10 nM K_d and to rFVa with ~100 nM K_d (Fig. 5 and Table 1). However, in SPR experiments, TFPI-2 bound to FV-1033 with ~36 nM K_d and to rFVa with ~252 nM K_d. The difference in K_d values using the two techniques could reflect the experimental approaches employed in each methodology. Further, in SPR experiments, TFPI-1 bound to FV-1033 with ~48 nM K_d and to rFVa with ~456 nM K_d (Fig. 5 and Table 1). In previous studies, pdFV bound to TFPI-1 with ~15 nM K_d (46).[6] Because pdFV and FV-1033 both contain all essential features for binding to TFPI-1 (57), the moderate variation in K_d previously observed with pdFV (46) and currently obtained with FV-1033 could reflect slight differences in the experimental conditions used in the two laboratories. Importantly, pull-down and Western blot analysis data presented in Fig. 6 demonstrate association of TFPI-2 with FV in plasma of pregnant women and with FV/Va_{AR} in platelets.

TFPI-1 and TFPI-2 compete with each other in binding to FV. In contrast, TFPI-1_{161} fails to compete, indicating that it does not bind to FV (Fig. 5*A*). These data confirm previous observations (47, 54, 56) and further suggest that, similar to TFPI-1, the C-terminal basic region of TFPI-2 plays an essential role in its interaction with FV. Our data are also consistent with the earlier observations that TFPI-1 binds to FVa (47) but with 10–20-fold reduced affinity (56). Whether or not the acidic residues (^{659}DDDEDS^{664} and/or ^{688}EDEESDADYD^{697}) in FVa (70) are involved in this interaction is not known. However, concentrations of full-length TFPI-1 (71) and TFPI-2 in platelets or plasma are quite low to appreciably bind to FVa, suggesting this interaction is not biologically significant.

Five basic amino acids (KRKRK) in the C-terminal region of TFPI-1 have been implicated in binding to the B-domain AR segment of FV_{AR}, a molecule that lacks the BR region (56). Because TFPI-1 and TFPI-2 compete with each other in binding to FV, and the C-terminal of TFPI-2 also has five conserved basic amino acids (KKKKK; Table 2), we predict that these residues bind to the FV-AR. Based on the ~20 nM K_d, only ~50% of ~0.5 nM TFPI-1 in plasma would be associated with FV. Similarly, based on the ~30 nM K_d, only ~40% or less of the ~7 nM TFPI-2 in pregnant women would be associated with FV. In contrast, based upon the ~0.1 nM K_d for TFPI-1 for FVa_{AR} present in platelets (56), a significant portion of TFPI-1 and by analogy TFPI-2 is expected to be associated with FVa_{AR}.[7]

TFPI-2 in platelets and in the plasma of pregnant women affects the hemostatic process. The primary effect observed in our assay system was on fibrinolysis (Fig. 7), whether the clotting was initiated with FXIa or with rTF. We observed ~40–50% inhibition of fibrinolysis specifically attributable to TFPI-2 whether platelets or plasma from pregnant women was used. When PRP was used (Fig. 7, *B* and *F*), the remaining antifibrinolytic activity could stem from the release of plasminogen activator inhibitor 1 and α_2-antiplasmin from platelets (44, 72, 73).

[6] Our efforts to obtain the K_d value for binding of pdFV to TFPI-2 or TFPI-1 using SPR were unsuccessful. The background binding to the CM5 chip in the absence of coupled TFPI-2 or TFPI-1 was extremely high, which precluded obtaining reliable data.

[7] We attempted purification of TFPI-2 from platelet lysates using an anhydroplasmin affinity column. After extensive washing with 50 mM Tris, 1 M NaCl, 2 mM $CaCl_2$, pH 7.5, the bound TFPI-2 was eluted with 10 mM HCl, 500 mM KCl, pH 2.1, in tubes containing 100 μl of 1 M Tris, pH 8.0, to a final volume of ~500 μl. However, Western blots of the HCl-eluted fractions revealed the presence of both TFPI-2 and FV/Va. These data indicate that TFPI-2 has very high affinity for platelet FV/Va.

TABLE 2

The conserved residue Lys-131 in Kunitz domain 3 and basic residues in the C-terminal region of TFPI-2 across mammalian species

The TFP-2 residues predicted to bind to FV-AR region are in boldface type. Corresponding residues in TFPI-1 predicted to participate in binding to the FV-AR region are ^{254}KTK**RKRKK**^{261} (56).

TFPI-2	Amino Acid Sequence		
Species	131 ↓	187 ↓	196 ↓
H. sapiens	PKKI	AKALKKKKKMPKL	
P. troglodytes	PKKI	AKALKKKKKMPKL	
M. mulatta	PKKI	AKALKRKKKIPKF	
P. abelii	PKKI	AKALRKKKKMPKL	
C. jacchus	PKKT	EKALKKQRKMPKI	
S. tridecemlineatus	PKKS	AKALKKGKKKKMP	
R. norvegicus	PRKS	VKALKKPKRRKIG	
M. musculus	PRKS	VKGWKKPKRWKIG	
S. scrofa	PKKG	VKALKKEKKMPRL	
C. familiaris	PKKS	VKALKKERNKKMT	
F. catus	PKKG	VKALKKEKNKKMP	
O. garnettii	PKKT	AKALKKEKNKTMP	
B. taurus	PKKA	VKALKKEKNKKMP	

Similarly, comparison of the antifibrinolytic activity of PPP from pregnant women (Fig. 7, *C* and *G*) and normal PPP supplemented with TFPI-2 (Fig. 7, *D* and *H*) indicates that the additional antifibrinolytic activity in pregnant women possibly stems from the increased levels of plasminogen activator inhibitors 1 and 2 and thrombin-activatable fibrinolysis inhibitor (74–76).

As expected, rTF was not inhibited by TFPI-2 in PRP (Fig. 7*F*) or PPP (Fig. 7*G*) from pregnant women; the increase in clot formation time in the case of PRP (Fig. 7*F*) could be due to TFPI-1 released from the platelets (71). Approximately 25% inhibition of FXIa could be attributed to TFPI-2 in PRP (Fig. 7*B*) or PPP (Fig. 7*C*) from pregnant women. The additional inhibition observed in the case of PRP (Fig. 7*B*) could stem from protease nexin-2 released from platelets (43, 77, 78). Although only ~25% inhibition of FXIa was observed during the first 5 min of the experiment (Fig. 7), inhibition of FXIa was expected to continue during the course of the experiment. Although we did not initiate intrinsic clotting through the activation of factor XII, we expected that TFPI-2 would efficiently inhibit the generated pKLK and FXIa in our experimental system. Thus, both intrinsic clotting and fibrinolysis are regulated by platelet TFPI-2 and by the TFPI-2 present in plasma of pregnant women.

Pregnant women are at risk for life-threatening hemorrhage during labor when the placenta is separated from the uterus, exposing large maternal arteries. These profound hemostatic challenges are overcome by local and systemic enhancement of coagulation and impairment of fibrinolysis. Plasma levels of several coagulation factors and fibrinolysis inhibitors are increased severalfold in pregnancy (74–76). In this context, TFPI-2 synthesized by the syncytiotrophoblasts (45) would provide additional antifibrinolytic activity during pregnancy/delivery to control bleeding.

In conclusion, platelet TFPI-2 plays an important role in the hemostatic process and adds to the list of other platelet factors, including polyphosphate (79), FV (80), protease nexin 1 and 2 (77, 78, 81), TFPI-1 (56), and plasminogen activator inhibitor-1 (72), that act as coagulant, anticoagulant, and antifibrinolytic agents. The effect of TFPI-2 on fibrinolysis is large and agrees with the K_i for plasmin being lower than for FXIa and pKLK. The data suggest a protective role of TFPI-2 against postpartum bleeding.

Acknowledgments—We thank Dr. Maureen Lynch for help in preparing the samples for immunohistochemistry; Dr. C. N. Rao for providing the TFPI-2 bacterial expression clone; Dr. George Broze for providing the TFPI-1 C terminus antibody; Dr. Carla Janzen for help in obtaining blood from pregnant women; and Drs. Amy Schmidt, Sriram Krishnaswamy, and Victor Marder for useful discussions.

REFERENCES

1. Broze, G. J., Jr., and Girard, T. J. (2012) Tissue factor pathway inhibitor: structure-function. *Front. Biosci.* **17,** 262–280
2. Sprecher, C. A., Kisiel, W., Mathewes, S., and Foster, D. C. (1994) Molecular cloning, expression, and partial characterization of a second human tissue-factor-pathway inhibitor. *Proc. Natl. Acad. Sci. U.S.A.* **91,** 3353–3357
3. Miyagi, Y., Koshikawa, N., Yasumitsu, H., Miyagi, E., Hirahara, F., Aoki, I., Misugi, K., Umeda, M., and Miyazaki, K. (1994) cDNA cloning and mRNA expression of a serine proteinase inhibitor secreted by cancer cells: identification as placental protein 5 and tissue factor pathway inhibitor-2. *J. Biochem.* **116,** 939–942
4. Rao, C. N., Reddy, P., Liu, Y., O'Toole, E., Reeder, D., Foster, D. C., Kisiel, W., and Woodley, D. T. (1996) Extracellular matrix-associated serine protease inhibitors (M_r 33,000, 31,000, and 27,000) are single-gene products with differential glycosylation: cDNA cloning of the 33-kDa inhibitor reveals its identity to tissue factor pathway inhibitor-2. *Arch. Biochem. Biophys.* **335,** 82–92
5. Petersen, L. C., Sprecher, C. A., Foster, D. C., Blumberg, H., Hamamoto, T., and Kisiel, W. (1996) Inhibitory properties of a novel human Kunitz-type protease inhibitor homologous to tissue factor pathway inhibitor. *Biochemistry* **35,** 266–272
6. Iino, M., Foster, D. C., and Kisiel, W. (1998) Quantification and characterization of human endothelial cell-derived tissue factor pathway inhibitor-2. *Arterioscler. Thromb. Vasc. Biol.* **18,** 40–46
7. Crawley, J. T., Goulding, D. A., Ferreira, V., Severs, N. J., and Lupu, F. (2002) Expression and localization of tissue factor pathway inhibitor-2 in normal and atherosclerotic human vessels. *Arterioscler. Thromb. Vasc. Biol.* **22,** 218–224
8. Chand, H. S., Foster, D. C., and Kisiel, W. (2005) Structure, function and biology of tissue factor pathway inhibitor-2. *Thromb. Haemost.* **94,** 1122–1130
9. Sierko, E., Wojtukiewicz, M. Z., and Kisiel, W. (2007) The role of tissue factor pathway inhibitor-2 in cancer biology. *Semin. Thromb. Hemost.* **33,** 653–659
10. Chand, H. S., Schmidt, A. E., Bajaj, S. P., and Kisiel, W. (2004) Structure-function analysis of the reactive site in the first Kunitz-type domain of human tissue factor pathway inhibitor-2. *J. Biol. Chem.* **279,** 17500–17507
11. Bajaj, M. S., Ogueli, G. I., Kumar, Y., Vadivel, K., Lawson, G., Shanker, S., Schmidt, A. E., and Bajaj, S. P. (2011) Engineering kunitz domain 1 (KD1) of human tissue factor pathway inhibitor-2 to selectively inhibit fibrinolysis: properties of KD1-L17R variant. *J. Biol. Chem.* **286,** 4329–4340
12. Kumar, Y., Vadivel, K., Schmidt, A. E., Ogueli, G. I., Ponnuraj, S. M., Rannulu, N., Loo, J. A., Bajaj, M. S., and Bajaj, S. P. (2014) Decoy plasminogen receptor containing a selective Kunitz-inhibitory domain. *Biochemistry* **53,** 505–517
13. Broze, G. J., Jr., Girard, T. J., and Novotny, W. F. (1990) Regulation of coagulation by a multivalent Kunitz-type inhibitor. *Biochemistry* **29,** 7539–7546
14. Castellino, F. J., and Ploplis, V. A. (2005) Structure and function of the

plasminogen/plasmin system. *Thromb. Haemost.* **93,** 647–654
15. Collen, D. (2001) Ham-Wasserman lecture: role of the plasminogen system in fibrin-homeostasis and tissue remodeling. *Hematology Am. Soc. Hematol. Educ. Program* **2001,** 1–9
16. Syrovets, T., Lunov, O., and Simmet, T. (2012) Plasmin as a proinflammatory cell activator. *J. Leukocyte Biol.* **92,** 509–519
17. Mignatti, P., and Rifkin, D. B. (1993) Biology and biochemistry of proteinases in tumor invasion. *Physiol. Rev.* **73,** 161–195
18. Miles, L. A., and Parmer, R. J. (2013) Plasminogen receptors: the first quarter century. *Semin. Thromb. Hemost.* **39,** 329–337
19. Miles, L. A., Dahlberg, C. M., Plescia, J., Felez, J., Kato, K., and Plow, E. F. (1991) Role of cell-surface lysines in plasminogen binding to cells: identification of α-enolase as a candidate plasminogen receptor. *Biochemistry* **30,** 1682–1691
20. Andronicos, N. M., Chen, E. I., Baik, N., Bai, H., Parmer, C. M., Kiosses, W. B., Kamps, M. P., Yates, J. R., 3rd, Parmer, R. J., and Miles, L. A. (2010) Proteomics-based discovery of a novel, structurally unique, and developmentally regulated plasminogen receptor, Plg-R-KT, a major regulator of cell surface plasminogen activation. *Blood* **115,** 1319–1330
21. Liotta, L. A., Goldfarb, R. H., Brundage, R., Siegal, G. P., Terranova, V., and Garbisa, S. (1981) Effect of plasminogen-activator (urokinase), plasmin, and thrombin on glycoprotein and collagenous components of basement-membrane. *Cancer Res.* **41,** 4629–4636
22. Festuccia, C., Dolo, V., Guerra, F., Violini, S., Muzi, P., Pavan, A., and Bologna, M. (1998) Plasminogen activator system modulates invasive capacity and proliferation in prostatic tumor cells. *Clin. Exp. Metastasis* **16,** 513–528
23. Rao, C. N., Liu, Y. Y., Peavey, C. L., and Woodley, D. T. (1995) Novel extracellular matrix-associated serine proteinase inhibitors from human skin fibroblasts. *Arch. Biochem. Biophys.* **317,** 311–314
24. Ortego, J., Escribano, J., and Coca-Prados, M. (1997) Gene expression of proteases and protease inhibitors in the human ciliary epithelium and ODM-2 cells. *Exp. Eye Res.* **65,** 289–299
25. Udagawa, K., Miyagi, Y., Hirahara, F., Miyagi, E., Nagashima, Y., Minaguchi, H., Misugi, K., Yasumitsu, H., and Miyazaki, K. (1998) Specific expression of PP5/TFPI2 mRNA by syncytiotrophoblasts in human placenta as revealed by *in situ* hybridization. *Placenta* **19,** 217–223
26. Sugiyama, T., Ishii, S., Yamamoto, J., Irie, R., Saito, K., Otuki, T., Wakamatsu, A., Suzuki, Y., Hio, Y., Ota, T., Nishikawa, T., Sugano, S., Masuho, Y., and Isogai, T. (2002) cDNA macroarray analysis of gene expression in synoviocytes stimulated with TNFα. *FEBS Lett.* **517,** 121–128
27. Rao, C. N., Cook, B., Liu, Y., Chilukuri, K., Stack, M. S., Foster, D. C., Kisiel, W., and Woodley, D. T. (1998) HT-1080 fibrosarcoma cell matrix degradation and invasion are inhibited by the matrix-associated serine protease inhibitor TFPI-2/33 kDa MSPI. *Int. J. Cancer* **76,** 749–756
28. Xu, C., Wang, H., He, H., Zheng, F., Chen, Y., Zhang, J., Lin, X., Ma, D., and Zhang, H. (2013) Low expression of TFPI-2 associated with poor survival outcome in patients with breast cancer. *BMC Cancer* **13,** 118
29. Wojtukiewicz, M. Z., Sierko, E., Zimnoch, L., Kozlowski, L., and Kisiel, W. (2003) Immunohistochemical localization of tissue factor pathway inhibitor-2 in human tumor tissue. *Thromb. Haemost.* **90,** 140–146
30. Chand, H. S., Du, X., Ma, D., Inzunza, H. D., Kamei, S., Foster, D., Brodie, S., and Kisiel, W. (2004) The effect of human tissue factor pathway inhibitor-2 on the growth and metastasis of fibrosarcoma tumors in athymic mice. *Blood* **103,** 1069–1077
31. Seppälä, M., Wahlström, T., and Bohn, H. (1979) Circulating levels and tissue localization of placental protein five (PP5) in pregnancy and trophoblastic disease: absence of PP5 expression in the malignant trophoblast. *Int. J. Cancer* **24,** 6–10
32. Bützow, R., Alfthan, H., Stenman, U. H., Suikkari, A. M., Bohn, H., and Seppälä, M. (1988) Immunofluorometric demonstration and quantification of placental protein 5 in the absence of pregnancy. *Clin. Chem.* **34,** 1591–1593
33. Obiekwe, B., Pendlebury, D. J., Gordeon, Y. B., Grudzinskas, J. G., Chard, T., and Bohn, H. (1979) The radioimmunoassay of placental protein 5 and circulating levels in maternal blood in the third trimester of normal pregnancy. *Clin. Chim. Acta* **95,** 509–516
34. Nisbet, A. D., Bremner, R. D., Herriot, R., Jandial, V., Horne, C. H., and Bohn, H. (1981) Placental protein 5 (PP5): development of a radioimmunoassay and measurement of circulating levels in normal pregnancy. *Br. J. Obstet. Gynaecol.* **88,** 484–491
35. Nisbet, A. D., Horne, C. H., Jandial, V., Bremner, R. D., Cruickshank, N., and Sutcliffe, R. G. (1982) Measurement of plasma placental proteins and estriol in the detection of intrauterine growth retardation. *Eur. J. Obstet. Gynecol. Reprod. Biol.* **13,** 333–342
36. Ogawa, M., Yanoma, S., Nagashima, Y., Okamoto, N., Ishikawa, H., Haruki, A., Miyagi, E., Takahashi, T., Hirahara, F., and Miyagi, Y. (2007) Paradoxical discrepancy between the serum level and the placental intensity of PP5/TFPI-2 in preeclampsia and/or intrauterine growth restriction: possible interaction and correlation with glypican-3 hold the key. *Placenta* **28,** 224–232
37. Arakawa, N., Miyagi, E., Nomura, A., Morita, E., Ino, Y., Ohtake, N., Miyagi, Y., Hirahara, F., and Hirano, H. (2013) Secretome-based identification of TFPI-2, a novel serum biomarker for detection of ovarian clear cell adenocarcinoma. *J. Proteome Res.* **12,** 4340–4350
38. Xiong, Y., Zhou, Q., Jiang, F., Zhou, S., Lou, Y., Guo, Q., Liang, W., Kong, D., Ma, D., and Li, X. (2010) Changes of plasma and placental tissue factor pathway inhibitor-2 in women with preeclampsia and normal pregnancy. *Thromb. Res.* **125,** e317–e322
39. Pan, J., Ma, D., Sun, F., Liang, W., Liu, R., Shen, W., Wang, H., Ji, Y., Hu, R., Liu, R., Luo, X., and Shi, H. (2013) Over-expression of TFPI-2 promotes atherosclerotic plaque stability by inhibiting MMPs in apoE(−/−) mice. *Int. J. Cardiol.* **168,** 1691–1697
40. Broos, K., De Meyer, S. F., Feys, H. B., Vanhoorelbeke, K., and Deckmyn, H. (2012) Blood platelet biochemistry. *Thromb. Res.* **129,** 245–249
41. Storti, F., van Kempen, T. H., and van de Vosse, F. N. (2014) A continuum model for platelet plug formation and growth. *Int. J. Numer. Method Biomed. Eng.* **30,** 634–658
42. Chung, D. W., Xu, W., and Davie, E. W. (2013) in *Hemostasis and Thrombosis*, 6th Ed. (Marder, V. J., Aired, W. C., Bennet, J. S., Schulman, S., and White G. C., II, eds) pp. 110–145, Lippincott Williams & Wilkins, Philadelphia
43. Walsh, P. N. (2013) in *Hemostasis and Thrombosis*, 6th Ed. (Marder, V. J., Aired, W. C., Bennet, J. S., Schulman, S., and White G. C., II, eds) pp. 468–474, Lippincott Williams & Wilkins, Philadelphia
44. Wiman, B., and Agren, A. (2013) in *Hemostasis and Thrombosis*, 6th Ed. (Marder, V. J., Aired, W. C., Bennet, J. S., Schulman, S., and White G. C., II, eds) pp. 334–340, Lippincott Williams & Wilkins, Philadelphia
45. Udagawa, K., Yasumitsu, H., Esaki, M., Sawada, H., Nagashima, Y., Aoki, I., Jin, M., Miyagi, E., Nakazawa, T., Hirahara, F., Miyazaki, K., and Miyagi, Y. (2002) Subcellular localization of PP5/TFPI-2 in human placenta: a possible role of PP5/TFPI-2 as an anti-coagulant on the surface of syncytiotrophoblasts. *Placenta* **23,** 145–153
46. Duckers, C., Simioni, P., Spiezia, L., Radu, C., Gavasso, S., Rosing, J., and Castoldi, E. (2008) Low plasma levels of tissue factor pathway inhibitor in patients with congenital factor V deficiency. *Blood* **112,** 3615–3623
47. Ndonwi, M., Girard, T. J., and Broze, G. J., Jr. (2012) The C-terminus of tissue factor pathway inhibitor α is required for its interaction with factors V and Va. *J. Thromb. Haemost.* **10,** 1944–1946
48. Mann, K. G., and Kalafatis, M. (2003) Factor V: a combination of Dr. Jekyll and Mr. Hyde. *Blood* **101,** 20–30
49. Camire, R. M., and Bos, M. H. (2009) The molecular basis of factor V and VIII procofactor activation. *J. Thromb. Haemost.* **7,** 1951–1961
50. Monkovic, D. D., and Tracy, P. B. (1990) Activation of human factor V by factor Xa and thrombin. *Biochemistry* **29,** 1118–1128
51. Thorelli, E., Kaufman, R. J., and Dahlbäck, B. (1997) Cleavage requirements for activation of factor V by factor Xa. *Eur. J. Biochem.* **247,** 12–20
52. Bos, M. H., and Camire, R. M. (2012) A bipartite autoinhibitory region within the B-domain suppresses function in factor V. *J. Biol. Chem.* **287,** 26342–26351
53. Bunce, M. W., Bos, M. H., Krishnaswamy, S., and Camire, R. M. (2013) Restoring the procofactor state of factor Va-like variants by complementation with B-domain peptides. *J. Biol. Chem.* **288,** 30151–30160
54. Vincent, L. M., Tran, S., Livaja, R., Bensend, T. A., Milewicz, D. M., and Dahlbäck, B. (2013) Coagulation factor V(A2440G) causes east Texas bleeding disorder via TFPIα. *J. Clin. Invest.* **123,** 3777–3787

55. Broze, G. J., Jr., and Girard, T. J. (2013) Factor V, tissue factor pathway inhibitor, and east Texas bleeding disorder. *J. Clin. Invest.* **123,** 3710–3712
56. Wood, J. P., Bunce, M. W., Maroney, S. A., Tracy, P. B., Camire, R. M., and Mast, A. E. (2013) Tissue factor pathway inhibitor-α inhibits prothrombinase during the initiation of blood coagulation. *Proc. Natl. Acad. Sci. U.S.A.* **110,** 17838–17843
57. Zhu, H., Toso, R., and Camire, R. M. (2007) Inhibitory sequences within the B-domain stabilize circulating factor V in an inactive state. *J. Biol. Chem.* **282,** 15033–15039
58. Rao, C. N., Reddy, P., Reeder, D. J., Liu, Y., Stack, S. M., Kisiel, W., and Woodley, D. T. (2000) Prokaryotic expression, purification, and reconstitution of biological activities (antiprotease, antitumor, and heparin-binding) for tissue factor pathway inhibitor-2. *Biochem. Biophys. Res. Commun.* **276,** 1286–1294
59. Girard, T. J., Warren, L. A., Novotny, W. F., Bejcek, B. E., Miletich, J. P., and Broze, G. J., Jr. (1989) Identification of the 1.4 kb and 4.0 kb messages for the lipoprotein associated coagulation inhibitor and expression of the encoded protein. *Thromb. Res.* **55,** 37–50
60. Zhong, D., Smith, K. J., Birktoft, J. J., and Bajaj, S. P. (1994) First epidermal growth factor-like domain of human blood coagulation factor IX is required for its activation by factor VIIa/tissue factor but not by factor XIa. *Proc. Natl. Acad. Sci. U.S.A.* **91,** 3574–3578
61. Bieth, J. G. (1984) *In vivo* significance of kinetic constants of protein proteinase-inhibitors. *Biochem. Med.* **32,** 387–397
62. Morrison, J. F., and Walsh, C. T. (1988) The behavior and significance of slow-binding enzyme-inhibitors. *Adv. Enzymol. Relat. Areas Mol. Biol.* **61,** 201–301
63. London, F., and Walsh, P. N. (1996) The role of electrostatic interactions in the assembly of the factor X activating complex on both activated platelets and negatively-charged phospholipid vesicles. *Biochemistry* **35,** 12146–12154
64. Isakari, Y., Sogo, S., Ishida, T., Kawakami, T., Ono, T., Taki, T., and Kiwada, H. (2009) Gene expression analysis during platelet-like particle production in phorbol myristate acetate-treated MEG-01 cells. *Biol. Pharm. Bull.* **32,** 354–358
65. Franks, D. J., Mroske, C., and Laneuville, O. (2001) A fluorescence microscopy method for quantifying levels of prostaglandin endoperoxide H synthase-1 and CD-41 in MEG-01 cells. *Biol. Proced. Online* **3,** 54–63
66. Biesiadecki, B. J., and Jin, J. P. (2011) A high-throughput solid-phase microplate protein-binding assay to investigate interactions between myofilament proteins. *J. Biomed. Biotechnol.* **2011,** 421701
67. Sperzel, M., and Huetter, J. (2007) Evaluation of aprotinin and tranexamic acid in different *in vitro* and *in vivo* models of fibrinolysis, coagulation and thrombus formation. *J. Thromb. Haemost.* **5,** 2113–2118
68. Laemmli, U. K. (1970) Cleavage of structural proteins during the assembly of the head of bacteriophage T4. *Nature* **227,** 680–685
69. Maroney, S. A., Haberichter, S. L., Friese, P., Collins, M. L., Ferrel, J. P., Dale, G. L., and Mast, A. E. (2007) Active tissue factor pathway inhibitor is expressed on the surface of coated platelets. *Blood* **109,** 1931–1937
70. Jenny, R. J., Pittman, D. D., Toole, J. J., Kriz, R. W., Aldape, R. A., Hewick, R. M., Kaufman, R. J., and Mann, K. G. (1987) Complete cDNA and derived amino acid sequence of human factor V. *Proc. Natl. Acad. Sci. U.S.A.* **84,** 4846–4850
71. Novotny, W. F., Girard, T. J., Miletich, J. P., and Broze, G. J., Jr. (1988) Platelets secrete a coagulation inhibitor functionally and antigenically similar to the lipoprotein associated coagulation inhibitor. *Blood* **72,** 2020–2025
72. Brogren, H., Karlsson, L., Andersson, M., Wang, L., Erlinge, D., and Jern, S. (2004) Platelets synthesize large amounts of active plasminogen activator inhibitor 1. *Blood* **104,** 3943–3948
73. Plow, E. F., and Collen, D. (1981) The presence and release of α2-antiplasmin from human platelets. *Blood* **58,** 1069–1074
74. Brenner B. (2004) Haemostatic changes in pregnancy. *Thromb. Res.* **114,** 409–414
75. Lockwood, C. J. (2006) Pregnancy-associated changes in the hemostatic system. *Clin. Obstet. Gynecol.* **49,** 836–843
76. Hale, S. A., Sobel, B., Benvenuto, A., Schonberg, A., Badger, G. J., and Bernstein, I. M. (2012) Coagulation and fibrinolytic system protein profiles in women with normal pregnancies and pregnancies complicated by hypertension. *Pregnancy Hypertens.* **2,** 152–157
77. Van Nostrand, W. E., Schmaier, A. H., Farrow, J. S., and Cunningham, D. D. (1990) Protease nexin-II (amyloid β-protein precursor): a platelet α-granule protein. *Science* **248,** 745–748
78. Smith, R. P., Higuchi, D. A., and Broze, G. J., Jr. (1990) Platelet coagulation factor XIa-inhibitor, a form of Alzheimer amyloid precursor protein. *Science* **248,** 1126–1128
79. Morrissey, J. H., Choi, S. H., and Smith, S. A. (2012) Polyphosphate: an ancient molecule that links platelets, coagulation, and inflammation. *Blood* **119,** 5972–5979
80. Thalji, N., and Camire, R. M. (2013) Parahemophilia: new insights into factor V deficiency. *Semin. Thromb. Hemost.* **39,** 607–612
81. Boulaftali, Y., Adam, F., Venisse, L., Ollivier, V., Richard, B., Taieb, S., Monard, D., Favier, R., Alessi, M. C., Bryckaert, M., Arocas, V., Jandrot-Perrus, M., and Bouton, M. C. (2010) Anticoagulant and antithrombotic properties of platelet protease nexin-1. *Blood* **115,** 97–106